

Comprehensive Report

Characterization of Airborne Dust Generated from the Grinding of Natural and Engineered Stone Products

Drew Thompson, PhD

Chaolong Qi, PhD, PE

Commander, U.S. Public Health Service

**Division of Field Studies and Engineering
Engineering and Physical Hazards Branch
EPHB Report No. 2023-DFSE-1489
October 2023**



Disclaimer

Mention of any company or product does not constitute endorsement by the National Institute for Occupational Safety and Health (NIOSH), Centers for Disease Control and Prevention (CDC).

In addition, citations to websites external to NIOSH do not constitute NIOSH endorsement of the sponsoring organizations or their programs or products. Furthermore, NIOSH is not responsible for the content of these websites. All Web addresses referenced in this document were accessible as of the publication date.

The findings and conclusions in this report are those of the authors and do not necessarily represent the official position of NIOSH, CDC.

Table of Contents

Abstract	v
Background	v
Assessment	v
Results.....	v
Conclusions and Recommendations.....	vi
Introduction.....	1
Background for Control Technology Studies	1
Background for this project.....	1
Background for this Study	3
Materials and Methods	4
Laboratory Testing System	4
Stone Product Samples	4
Test Conditions	5
Sampling Methods	6
Results.....	8
Crystalline Silica Content in Respirable and Bulk Dust Samples	8
Respirable Dust and Crystalline Silica Normalized Generation Rates	9
Volume Removal Rates.....	12
Particle Size Distributions	14
Discussion	17
Comparison of Crystalline Silica Content.....	17
Comparison of Particle Size Distribution	18
Comparison of Generation Rate	18
Limitations and Implications of the Experiment Results	19
Conclusions and Recommendations.....	20
References	21
Appendices	26
Appendix I. Treatment of APS Data.....	26
Appendix II. Additional Tables and Figures	30
Appendix III. Tabulated Data from Figures	31

Appendix IV. Respirable Sample Dataset 40

Abstract

Background

Workplace exposure to respirable crystalline silica (RCS) can cause silicosis, a progressive lung disease marked by scarring and thickening of the lung tissue. Crystalline silica is found in several materials, such as brick, block, mortar, and concrete. Construction and manufacturing tasks that cut, break, grind, abrade, or drill those materials have been associated with overexposure to dust containing RCS. Stone countertop products can contain various levels of crystalline silica (can be >90 wt%) and working with this material during stone countertop fabrication has been shown to cause excessive RCS exposures. NIOSH scientists are conducting a study to develop a control strategy for workers' RCS exposure during stone countertop fabrication. The laboratory research described in this report is part of that study.

Assessment

NIOSH scientists systematically characterized the airborne dust generated from grinding engineered and natural stone products using a laboratory testing system designed and operated to collect representative respirable dust samples. The laboratory experiments in this study determined dust and crystalline silica generation rates, dust size distributions, and crystalline silica content during the dry grinding of nine stone countertop products including seven engineered stones containing crystalline silica in a polymer resin matrix from five major manufacturers (labeled Stone A, B, and 1 through 5 throughout), one engineered stone containing recycled glass in a Portland cement matrix (Stone C), and one natural stone, granite.

Results

For each stone product, the corresponding crystalline silica content in bulk dust samples and respirable dust samples were found to be similar. The crystalline silica content in the respirable dust was within or below the ranges reported in the manufacturers' safety data sheets for each of the respective stone products. It is worth noting that no crystalline silica was detected in Stone C. In addition, Stone B, whose new formulation was advertised by the manufacturer as having a reduced crystalline silica content (≤ 50 wt%) with respect to their previous formulation, had a crystalline silica content comparable to that of the granite evaluated in this study (about 20-30 wt%).

Since sample thickness may influence the rate at which material is removed from the stone product sample during grinding, the normalized generation rate results from differing sample thickness are presented separately. Among the four stone products with samples about 30 mm thick, the mean normalized generation rates of respirable dust ranged from 24 to 43 mg cm⁻³ with granite being the highest and Stones A, B, and C being comparable. The mean normalized generation rates of RCS for these samples ranged from 0.0 to 16 mg cm⁻³ with Stone A being the highest followed by granite, Stone B, and finally Stone C which generated no

detectable crystalline silica. Among the five engineered stone products with a resin matrix and sample thicknesses of around 20 mm, mean normalized generation rates of respirable dust and RCS both remain in relatively narrow ranges.

The mass-based distributions showed the most prominent modes at 5.1 – 8.0 μm for all the stone products evaluated in this study. This suggests that the mechanical process of the fabrication task, in this case a pneumatic angle grinder equipped with a coarse diamond grinding cup wheel, rather than the type of stone product predominantly determines the shape of the dust size distribution. The results of particle size distribution and RCS generation rate both contributed to the observation published previously that the highest normalized generation rate of RCS consistently occurred at 3.2 – 5.6 μm for all the stones containing crystalline silica.

Conclusions and Recommendations

Workers are likely to be exposed to lower concentrations of RCS when working with engineered stones containing no crystalline silica (e.g., Stone C), followed by engineered stones specifically designed with lower silica content (e.g., Stone B), then granite similar to the one in this study, and finally engineered stones that contain high silica content (up to about 90 wt% in a resin matrix). Working with the engineered stones from different manufacturers that have similar thicknesses and colors and contain similarly high levels of silica content is likely to lead to similar levels of RCS exposure for workers.

Thus, following the hierarchy of controls, a layered, overall control strategy can incorporate elimination (e.g., products similar to Stone C), substitution (e.g., products similar to Stone B), and engineering controls at the top to minimize workers' RCS exposure during stone countertop fabrication. For developing engineering controls, prioritizing the removal of particles in the range of 3.2 – 5.6 μm near the generation sources should help maximize RCS reduction, since the highest normalized generation rate of RCS consistently occurred in this size range for all the stones containing crystalline silica in this study.

Introduction

Background for Control Technology Studies

The National Institute for Occupational Safety and Health (NIOSH) is the primary Federal agency engaged in occupational safety and health research. Located in the Department of Health and Human Services, it was established by the Occupational Safety and Health Act of 1970. This legislation mandated NIOSH to conduct a number of research and education programs separate from the standard setting and enforcement functions carried out by the Occupational Safety and Health Administration (OSHA) in the Department of Labor. An important area of NIOSH research deals with methods for controlling occupational exposure to potential chemical and physical hazards. The Engineering and Physical Hazards Branch (EPHB) of the Division of Field Studies and Engineering has been given the lead within NIOSH to study the engineering aspects of health hazard prevention and control.

Since 1976, EPHB has conducted assessments of health hazard control technologies on the basis of industry, common industrial process, or specific control techniques. Examples of these completed studies include the foundry industry; various chemical manufacturing or processing operations; spray painting; and the recirculation of exhaust air. The objective of each of these studies has been to document and evaluate effective control techniques for potential health hazards in the industry or process of interest, and to create a more general awareness of the need for, or availability of, an effective system of hazard control.

These studies involve a number of steps or phases. Initially, a series of walk-through surveys is conducted to select plants or processes with effective and potentially transferable control concept techniques. Next, in-depth surveys are conducted to determine both the control parameters and the effectiveness of these controls. The reports from these in-depth surveys are then used as a basis for preparing technical reports and journal articles on effective hazard control measures. Ultimately, the information from these research activities builds the data base of publicly available information on hazard control techniques for use by health professionals who are responsible for preventing occupational illness and injury.

Background for this Project

Crystalline silica refers to a group of minerals composed of silicon and oxygen; a crystalline structure is one in which the atoms are arranged in a repeating three-dimensional pattern [Bureau of Mines, 1992]. The three major forms of crystalline silica are quartz, cristobalite, and tridymite; quartz is the most common form [Bureau of Mines, 1992]. Respirable crystalline silica (RCS) refers to that portion of airborne crystalline silica dust that is capable of entering the gas-exchange regions of the lungs if inhaled; this includes particles with aerodynamic diameters less than approximately 10 micrometers (μm) [NIOSH, 2002]. Silicosis, a fibrotic disease of the lungs, is an occupational respiratory disease caused by the inhalation and

deposition of RCS dust [NIOSH, 1986]. Silicosis is irreversible, often progressive (even after exposure has ceased), and potentially fatal. Because no effective treatment exists for silicosis, prevention through exposure control is essential.

Stone countertops became increasingly popular among consumers in recent years. Granite and engineered quartz stone are the two major stone countertop materials, respectively representing an estimated 27% and 8% market share (by sales) in a \$74B global countertop market in 2012. Rose et al. [2019] reported that there were an estimated 8,694 establishments and 96,366 employees in the stone fabrication industry in the United States in 2018 by analyzing data from the Bureau of Labor Statistics.

Unfortunately, a large amount of dust that contains RCS can be produced during stone countertop fabrication and installation. On average, granite naturally contains 72 wt% crystalline silica by weight [Blatt and Tracy, 1997], and engineered quartz stone contains about 90 wt% quartz grains by mass in a polymer matrix [Phillips et al., 2013]. An outbreak of silicosis was reported in Israel [Kramer et al., 2012], where 25 patients were identified who shared an exposure history of having worked with engineered quartz stone countertops without dust control or respiratory protection. In addition, 46 silicosis cases were reported in Spain among men working in the stone countertop cutting, shaping, and finishing industry [Pérez-Alonso et al., 2014]. In 2015, the first silicosis case in the US was reported for a worker who had worked with engineered quartz stone countertops [Friedman et al., 2015]; and NIOSH and OSHA [2015] released a Hazard Alert on worker exposure to silica during countertop manufacturing, finishing and installation. More recently, Rose et al. [2019] reported 18 silicosis cases, including two fatalities, among workers in the stone fabrication industry in California, Colorado, Texas, and Washington of the US; and Fazio et al. [2023] reported 52 silicosis cases, including 10 fatalities, in the state of California. A systematic evaluation, optimization, and improvement of engineering control measures for processes involved in stone countertop fabrication and installation is needed to give manufacturers, fabricators, and occupational safety and health professionals best-practice recommendations for consistently reducing RCS exposures below the NIOSH Recommended Exposure Limit (REL) of 0.05 mg/m³ (50 µg/m³).

A review of workplace inspections conducted by the state of Washington's Department of Labor and Industries found overexposures to RCS (above the OSHA Permissible Exposure Limit (PEL)) and violation of rules on engineering controls in 9 of 18 stone countertop shops inspected [Lofgren, 2008]. Data from the OSHA's Integrated Management Information System (IMIS) reveals that citations issued for exceeding the PEL for RCS jumped from an average of 4 per year during 2000-2002 to an average of 59 per year during 2003-2011 at stone countertop fabrication shops and installation sites. These results indicate that dust control methods did not appear to be well implemented among shops in this industry. OSHA published a new PEL of 0.05 mg/m³ (50 µg/m³) as an 8-hr time weighted average (TWA) for RCS [81 Fed. Reg. 16285, 2016], making it critical to address these overexposures.

This project aims at reducing workers' exposures and risks in the stone countertop fabrication and installation industries by evaluating, optimizing, and improving engineering control measures, evaluating their effectiveness through field studies, and disseminating the results through NIOSH field survey reports, articles in professional and trade journals, and a NIOSH Internet topic page. The long-term objective of this study is to provide practical recommendations for effective dust controls that will prevent overexposures to RCS during stone countertop fabrication and installation.

Background for this Study

In a survey of 47 granite countertop fabrication shops in Oklahoma, 15% of shops reported using dry methods for edge grinding most of the time [Phillips and Johnson, 2012]. This value is similar to the findings of Glass et al. [2022] where 16% of the 324 participants in the engineered stone fabrication industry in Victoria, Australia spent more than 50% of the time doing dry work in their most recent jobs. Field studies by the NIOSH [NIOSH, 2016a; NIOSH, 2016b; NIOSH, 2016c] in relatively large stone countertop fabrication shops found that cutting was mostly performed by machines operated remotely, such as bridge saws or water-jet cutters, but final grinding of the stone edge profiles was exclusively conducted by workers using hand-held grinders. Those grinding tasks led to the highest RCS exposure among workers in these shops. The NIOSH studies reported overexposure to RCS for the workers conducting grinding and some polishing tasks in these shops, even when regular wet methods were employed. A recent NIOSH study [2021] reported that the RCS exposure for workers conducting grinding tasks can be reduced to levels below the OSHA PEL by supplementing the regular wet methods incorporated in the grinders with a sheet-water-wetting method. There is a need for additional or more effective engineering controls to consistently reduce RCS exposures to permissible levels.

When developing effective and feasible engineering controls, dust and crystalline silica generation rates, dust size distribution, and size-dependent crystalline silica content are valuable information [Qi et al., 2016]. This characterization is best done systematically in a well-controlled laboratory test system. Of the four tasks identified by Phillips et al. [2013] as having the highest estimated RCS exposures (dry sweeping, dry cutting, dry grinding, and dry polishing), only the cutting and polishing of engineered stone have been characterized in a laboratory using one or more of the metrics highlighted above. To the best of our knowledge, no prior laboratory study has been conducted to characterize the dust generated from grinding stone countertop products. Therefore, this study was to characterize the dust generated during the dry grinding of engineered and natural stones inside a controlled laboratory testing system by following a standard method to determine dust and crystalline silica generation rates, dust size distributions, and crystalline silica content. The results obtained will serve as the basis to (i) identify stone products currently available that potentially lower or eliminate RCS exposure, (ii) develop potential engineering control measures and, (iii) evaluate engineering control effectiveness by comparing the reduced generation rates obtained from the same standard method.

Materials and Methods

Laboratory Testing System

The laboratory testing system used in this study was designed and operated to comply with European Standard EN 1093-3 [CEN, 2006] and is given in Figure 1. The system consisted of an enclosed chamber where the airborne dust was generated, a funnel, and a duct where the airborne dust was sampled. A house ventilation system equipped with a variable-speed blower drew room air into the test system through pre- and HEPA filters at a flow rate of $0.17 \text{ m}^3 \text{ s}^{-1}$. The flow rate was monitored by a micromanometer (Airflow™ MEDM 500, Airflow Developments LTD., UK) connected to a delta tube (306AM-11-AO, Midwest instruments, USA) which functioned as an averaging pitot tube. Under the operating flow rate used in this study, the average flow velocity in the chamber was 0.11 m s^{-1} which meets the standard's requirement that the average flow be larger than or equal to 0.1 m s^{-1} for the transport of respirable dust. The Reynolds numbers for the chamber and duct were 9,100 and 46,000, respectively, indicating that the flow was turbulent. Turbulent flow causes aerosol mixing and allows for the collection of representative samples in the sampling section. After the sampling section, air was passed through the filter cartridges inside an air handling unit (PSKB-1440, ProVent LLC, USA) that was not driving airflow before discharging into the house ventilation duct.

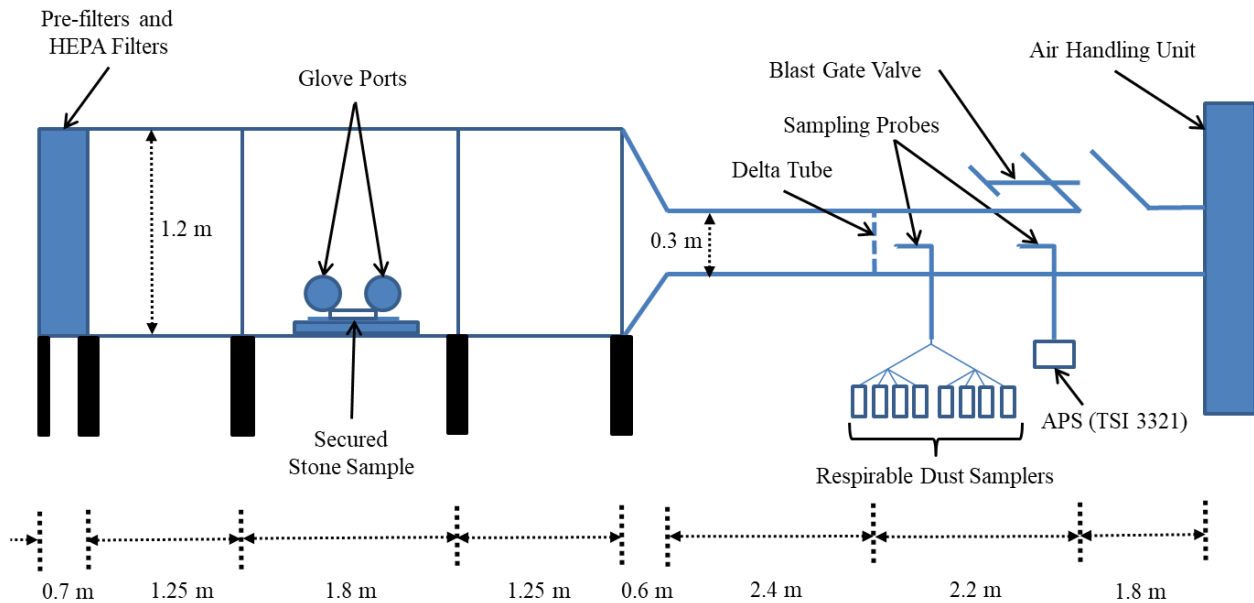


Figure 1. Diagram of the laboratory testing system

Stone Product Samples

We did a search of media-reports and market data on engineered stone products and identified nine representative stone products to investigate in this study: seven engineered stones containing crystalline silica in a polymer resin matrix from five

major manufacturers (labeled Stones A, B, 1 through 5), one engineered stone containing recycled glass in a Portland cement matrix (Stone C), and one natural stone, granite. According to their safety data sheets (SDS), engineered stone products Stone A and Stones 1 through 5 were composed largely of crystalline silica, up to about 90 wt%, in a resin matrix with additives such as pigments and other minerals. Stone B was made using a new formula with a crystalline silica content of less than 50 wt%, per the SDS. For Stone C, with glass being amorphous silica, the crystalline silica should have been limited to the minute amounts present in the cement matrix. The SDS listed a crystalline silica content of less than 0.2 wt%. The importer of the Granite sample listed an estimated crystalline silica content of up to 72 wt% in the SDS. All stone product samples had a white or light-colored coloring to minimize a potential interference from pigments for different colors. To ensure similar contact surfaces between the stone sample’s edge and the grinding cup wheel, we attempted a best effort to maintain the stone sample thickness as constant as possible. In some instances, this required clamping several substrates of the same stone together. The samples for Granite and Stones A through C had a thickness of approximately 30 mm and were studied June 14 – August 2, 2021. Stones 1 through 5 had a thickness of approximately 20 mm and were studied March 7 – 18, 2022. The stone product sample name, manufacturer reported crystalline silica content, sample thickness, number of substrates per sample, and measured material density are summarized in Table 1.

Table 1. Summary of stone product properties

Stone	Crystalline silica content (wt%) reported in SDS	Thickness (mm)	Number of substrates per sample	Material density, ρ_m (kg m ⁻³)
Granite	0 – 72	29	3	2600
A	70 – 90	30	7	2100
B	1 – 50	32	7	2100
C	< 0.2	32	1	2300
1	24 – 93	19	1	2200
2	> 87	20	1	2300
3	80 – 95	20	1	2300
4	70 – 90	19	1	2100
5	≤ 93	20	1	2200

Test Conditions

A hand-held pneumatic angle grinder (GPW-216, Gison Machinery Co., Ltd., Taiwan) equipped with a 10 cm diameter, coarse, diamond grinding cup wheel (Model SIS-4SPCW-SC, Stone Industrial Supplies, Inc., USA) was manually operated through the chamber’s glove ports. Three experimental runs were completed for each stone product. In the experimental runs for Granite and Stones A through C, two operators alternated grinding the stone samples for 4 min each. All but one run had 8 min of active grinding. The second run for Stone C had 16

min of active grinding. In the experimental runs for Stones 1 through 5, the same two operators alternated grinding the stone samples, with one operator grinding on the first and third runs and the other operator on the second run. Samples were grinded for 4 min in each run, except for the second run for Stone 1 where the sample was grinded for approximately 4.7 min.

Before and after each experimental run, stone samples were weighed on a scale with 2 g certified readability (Model D51XW10WR3, OHAUS Corp., USA) to determine the mass removed during the specific experimental run. A volume removal rate was calculated from the mass removed, material density, and duration of grinding. After the completion of three experimental runs for each stone, we collected bulk dust samples from the dust settled on the floor of the testing chamber for analysis. Then the testing chamber was thoroughly cleaned to prevent sample cross-contamination.

Sampling Methods

Two isoaxial sampling probes extracted aerosols from the duct of the testing system to (a) up to eight respirable dust samplers operated in parallel and (b) an Aerodynamic Particle Sizer (APS) Spectrometer (Model 3321, TSI Inc., USA). The sampling probes were near-isokinetic and estimated to have less than 10% sampling bias for particles smaller than 11 μm by following Brockmann [2011]. Probes were connected to their respective samplers and instrumentation using metallic fittings and Tygon[®] or conductive silicone tubing to minimize particle losses caused by electrostatic effects. The respirable dust sampler aerosol flow was split by first passing through a wye fitting followed by a 4-way flow splitter (Model 3708, TSI Inc., USA) on both branches. The overall sampling biases of the sampling trains were estimated to be less than 10% for particles with diameters ranging from 5 nm to 9 μm [Thompson and Qi, 2023].

GK 4.162 RASCAL Cyclones (Mesa Laboratories, Inc., USA) operated at a flow rate of 9.0 l min⁻¹ were used to collect respirable dust on 47 mm diameter, 5 μm pore size, polyvinyl chloride (PVC) filters backed by cellulose support pads in three-piece conductive cassettes following NIOSH Methods 0600 and 7500 [NIOSH, 1998; NIOSH, 2003]. The sampling flow rates for the respirable samplers were provided by Leland Legacy Sample Pumps (SKC Inc., USA). The following number of respirable samples were collected in parallel from each experimental run: 6 samples for Stones 1 through 5; 1 sample for the first experimental run of Stone C; and 2 samples for Granite, Stone A, Stone B, and the remaining experimental runs of Stone C. See Figure 7 in Appendix II for a schematic of the differing sampling train configurations for the respirable samplers in each experimental run.

PVC filters were pre-weighed and post-weighed to determine respirable dust mass collected. Crystalline silica analysis of each bulk dust and air sample was performed by x-ray diffraction (XRD) in accordance with NIOSH Method 7500 [NIOSH, 2003] to quantify the amount of quartz, cristobalite, and tridymite forms of crystalline silica present. The PVC filters from all the air samples were processed by muffle furnace ashing for sample preparation to minimize the potential underestimation of

crystalline silica caused by tetrahydrofuran (THF) for sample preparation [Qi et al., 2022]. Depending on analytical instruments, analysts, and XRD interferences from feldspar or between silica polymorphs, limits of detection (LOD) for each analyte were as listed in Table 2. Limits of quantification (LOQ) were calculated as 10/3 times the LOD.

Table 2. Limits of detection (LOD) for the analysis of air and bulk samples

Analyte	Air samples ($\mu\text{g sample}^{-1}$)	Bulk samples (%wt)
Respirable dust	20 – 40	–
Cristobalite	5 – 100	0.2 – 4
Quartz	5 – 10	0.2 – 0.7
Tridymite	10 – 100	0.5 – 3

From the mass of the dust and crystalline silica of each sample, we calculated the crystalline silica content and the normalized generation rate. Crystalline silica content was defined as the percent crystalline silica by weight. The normalized generation rate, G , represented the mass of airborne respirable dust or RCS generated per unit of volume removed from the stone sample during grinding and is defined by Equation 1, where ρ_m is the bulk material density of the stone sample, m_{sampl} is the mass collected by the respirable sampler, m_{remov} is the mass removed from the stone sample, and Q and Q_{sampl} are the nominal flow rates of the test chamber and respirable sampler, respectively.

$$G = \frac{Q\rho_m m_{sampl}}{Q_{sampl}m_{remov}} \quad \text{Equation 1}$$

Crystalline silica content and normalized generation rate are not measured directly, but instead determined through other quantities via functional relationships. Thus, the combined standard uncertainty for uncorrelated input quantities, as defined in Equation 2, was used to estimate the standard deviation by following the approach of International Organization for Standardization [2008]:

$$u_c(y) = \sqrt{\sum_{i=1}^N \left(\frac{\partial f}{\partial x_i}\right)^2 u^2(x_i)} \quad \text{Equation 2}$$

where f is the functional relationship, x_i is the arithmetic mean of mass measurement i (dust, quartz, cristobalite, or tridymite), $u(x_i)$ is the standard uncertainty of mass measurement i , N is the number of mass measurements, and $\partial f/\partial x_i$ is evaluated at x_i .

The size distributions of particles with aerodynamic diameters ranging from 0.5 to 20 μm were measured every 1 s by the APS. A correction was applied in the Aerosol Instrument Manager (AIM) (v10.2.0.11, TSI Inc., USA) software package to improve APS sizing accuracy for particles with densities that aren't close to unit density, $1000 \pm 100 \text{ kg m}^{-3}$ [Wang and John, 1987; TSI Incorporated, 2013]. See Appendix I for more details. Number and mass-based particle size distributions

representative of the stone grinding process were obtained from the APS. To account for transients due to particle transport in the testing system, the periods of active grinding were identified as those having the highest moving average of particle number concentration over the nominal grinding duration. For each engineered stone product, the particle number and mass distributions were calculated from the APS data collected each second during periods of active grinding. Trimodal lognormal size distribution functions were fit to APS-measured particle number distributions following the procedure outlined in Appendix I.

Results

Crystalline Silica Content in Respirable and Bulk Dust Samples

Respirable and bulk dust samples from Stones A, B, 1, 2, 4, and 5 contained cristobalite and quartz forms of crystalline silica. Only the quartz form was detected in the Granite and Stone 3. No tridymite was detected in any sample. No crystalline silica was detected in Stone C. The crystalline silica content in respirable dust is presented in Figure 2 (see Table 6 in Appendix III for the tabulated data in this figure, in addition to the combined standard uncertainties of cristobalite and quartz content). In general, all engineered stone products containing crystalline silica in a resin matrix, excluding Stone B, had a mean crystalline silica content respirable dust ranging from 57 to 75 wt%. Stone B, whose new formulation was claimed by the manufacturer as having a lower crystalline silica content, was found to have a crystalline silica content comparable to that of the Granite (about 25 wt%).

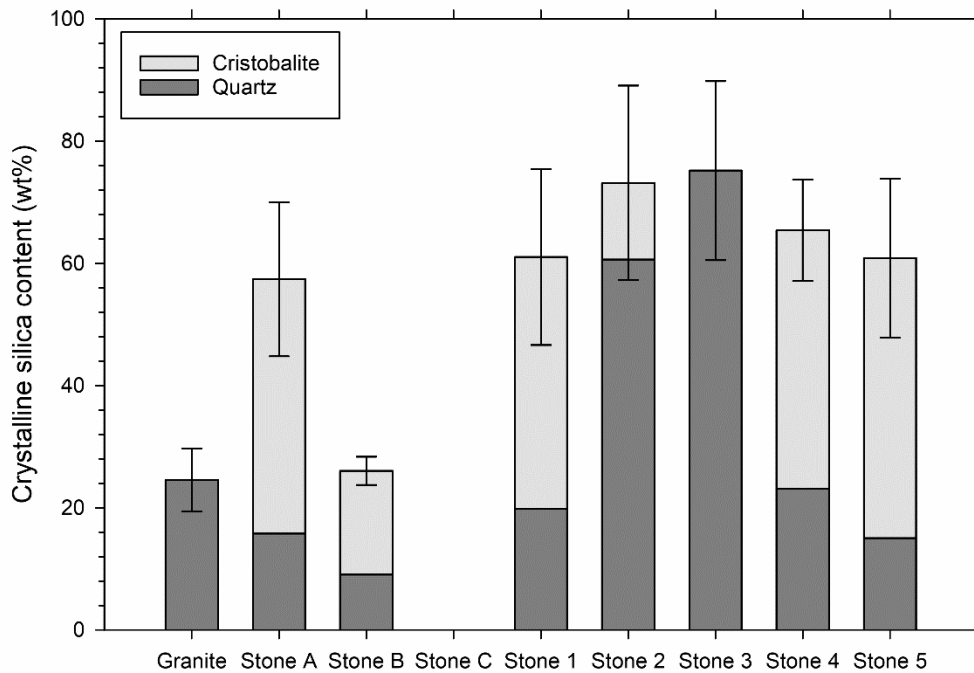


Figure 2. Crystalline silica content of respirable dust. Shadings represent the fraction of cristobalite and quartz forms. Error bars represent the combined standard uncertainty of crystalline silica content.

As seen in Table 3, the crystalline silica content of bulk dust samples was similar to that seen in the respirable dust for each stone product, and they were mostly in agreement with the manufacturers’ reported ranges for the respective stone product as listed in Table 1.

Table 3. Crystalline silica content of bulk dust

Stone	Cristobalite (wt%)	Quartz (wt%)	Crystalline silica (wt%)
Granite	0.0	30	30
A	46	14	60
B	12	11	23
C	0.0	0.0	0.0
1	32	33	65
2	21	60	81
3	0.0	> 95	> 95
4	45	25	70
5	30	38	68

Respirable Dust and Crystalline Silica Normalized Generation Rates

The mean normalized generation rates of respirable dust and RCS from the grinding of stone products are plotted in Figure 3. As will be elaborated in more detail in the Discussion section, sample thickness, among other factors, may influence the rate

at which material is removed from the stone product sample during grinding. This will in turn affect the normalized generation rates. Because of this, we will present the normalized generation rate results from differing sample thickness separately, and the two groups of data should not be directly compared against each other.

The four stone products studied in the summer of 2021 all had samples that were about 30 mm thick. For these samples, the mean normalized generation rates of respirable dust ranged from 24 to 43 mg cm⁻³ with Granite being the highest and Stones A, B, and C being comparable, as seen in Figure 3(a). The mean normalized generation rates of RCS for these samples ranged from 0.0 to 16 mg cm⁻³ with Stone A being the highest followed by Granite, Stone B, and finally Stone C which generated no detectable crystalline silica.

The five engineered stone products with a resin matrix studied in the spring of 2022 had sample thicknesses of around 20 mm. Mean normalized generation rates of respirable dust for each engineered stone product ranged from 7.6 to 13 mg cm⁻³ and are plotted in Figure 3(b). Stone 4 had the highest mean normalized generation rate of respirable dust, followed by, in decreasing order, Stone 1, 2, 5, and 3. Mean normalized generation rates of RCS from these engineered stone products ranged from 5.6 to 8.4 mg cm⁻³ and ranked, in decreasing order, as follows: Stone 4, 1, 2, 3, and 5.

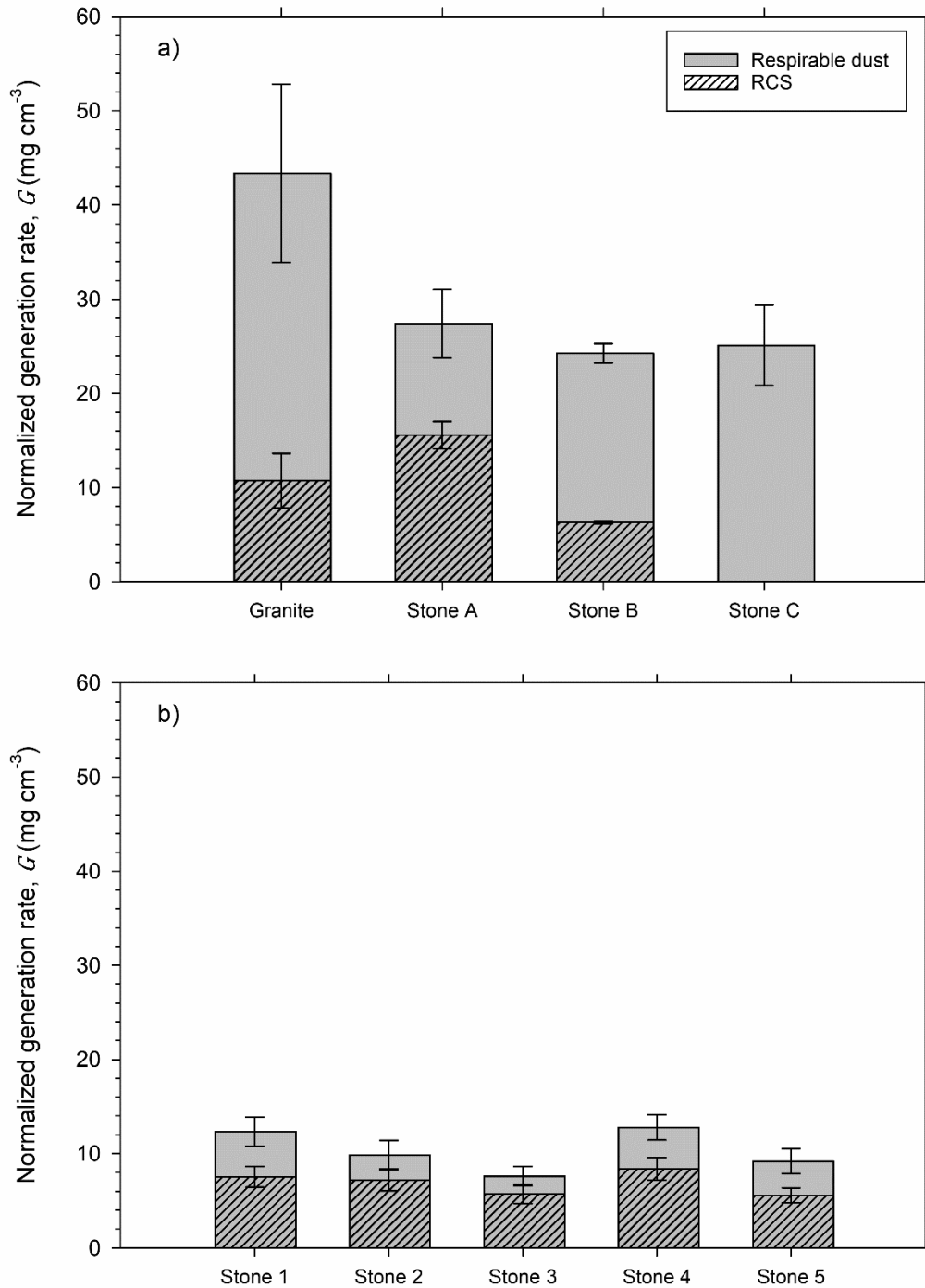


Figure 3. Respirable dust and RCS normalized generation rates for grinding ~30 mm thick samples of Granite and Stones A – C in (a) and ~20 mm thick samples of Stones 1 – 5 in (b). Each datum represents the mass of dust or crystalline silica (units of mg) normalized by the volume removed from the stone sample during grinding (units of cm³). Error bars represent the combined standard uncertainty of the normalized generation rate.

Volume Removal Rates

Mean volume removal rates from the grinding of stone products are shown in Figure 4. Like the normalized generation rates, we will present the volume removal rates separately for differing stone product sample thicknesses. For the four stone products with a sample thickness of approximately 30 mm, as shown in Figure 4(a), the mean volume removal rates ranged from 5.2 to 10 cm³ min⁻¹ and were ranked, in decreasing order: Stone C, Stone B, Granite, and Stone A. For the five engineered stone product samples with a thickness of about 20 mm, plotted in Figure 4(b), the mean volume removal rates ranged from 7.9 to 11 cm³ min⁻¹ and were ranked, in decreasing order: Stone 4, 1, 2, 5, and 3.

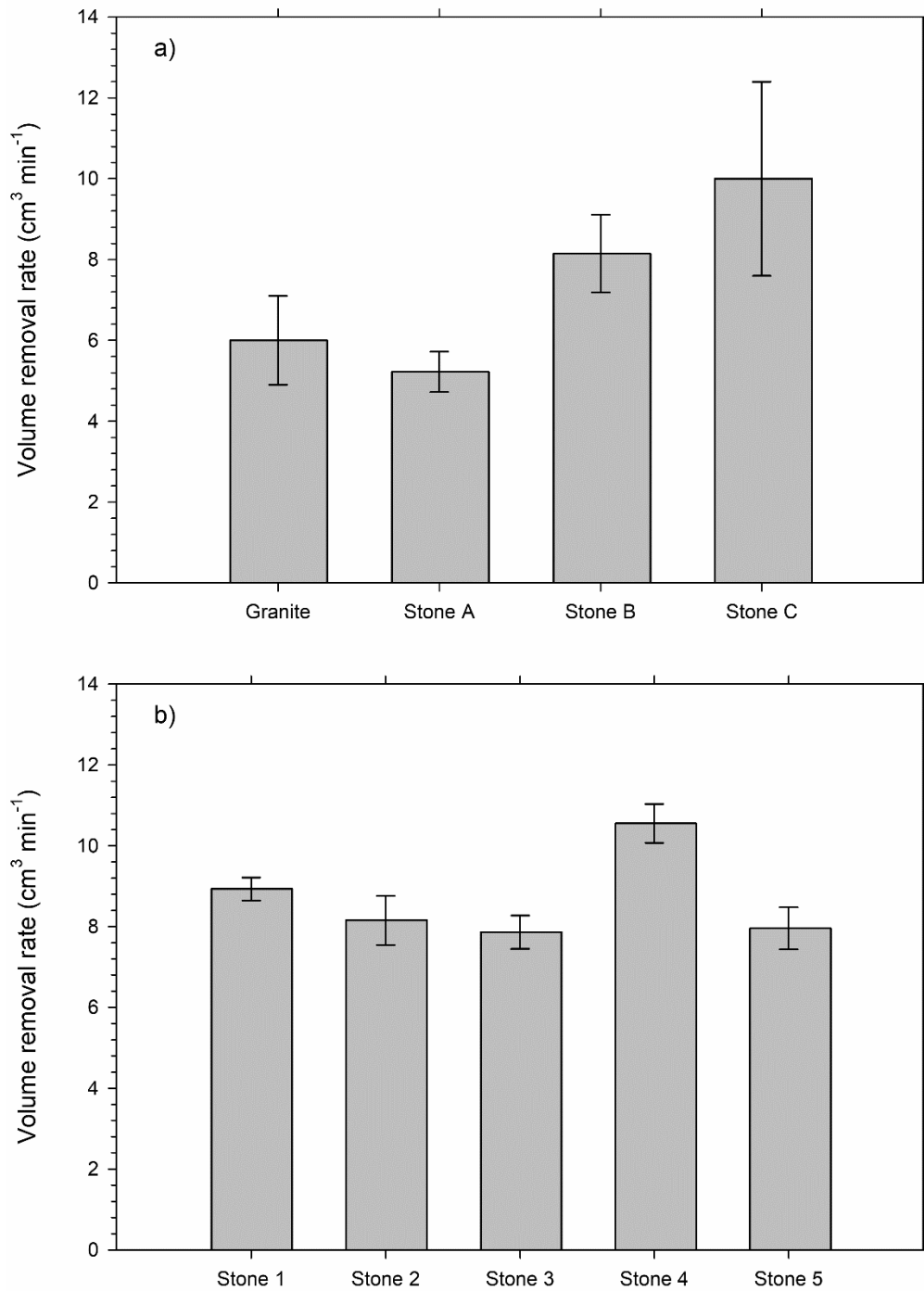
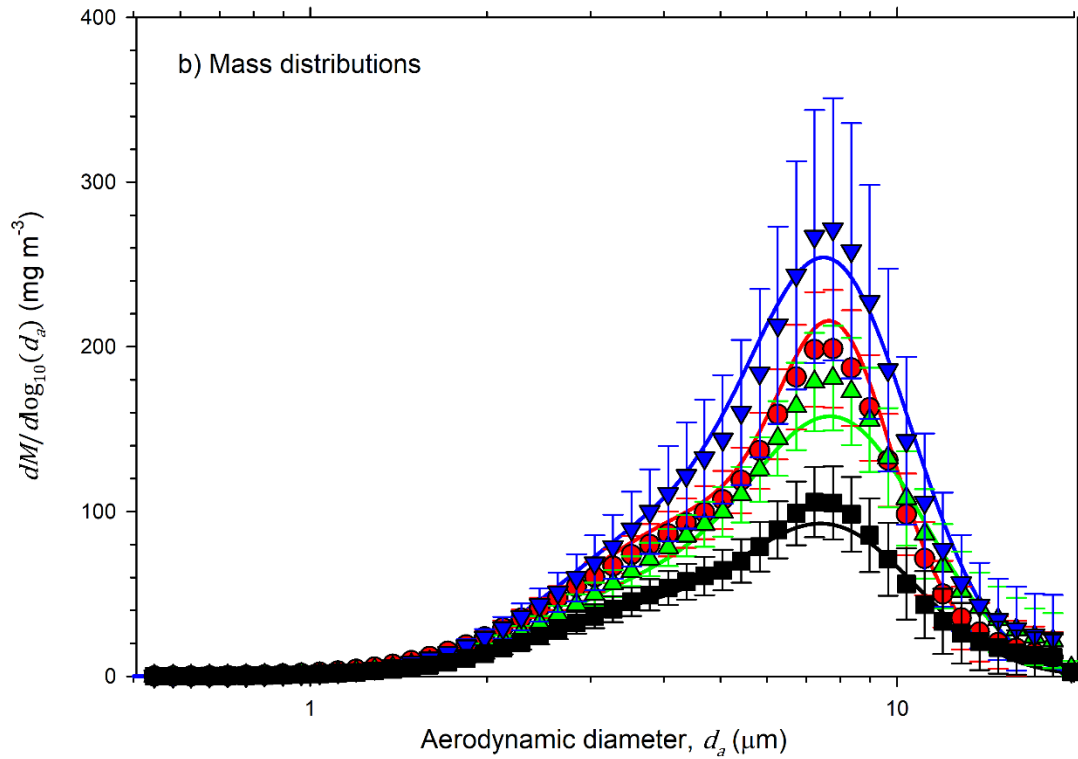
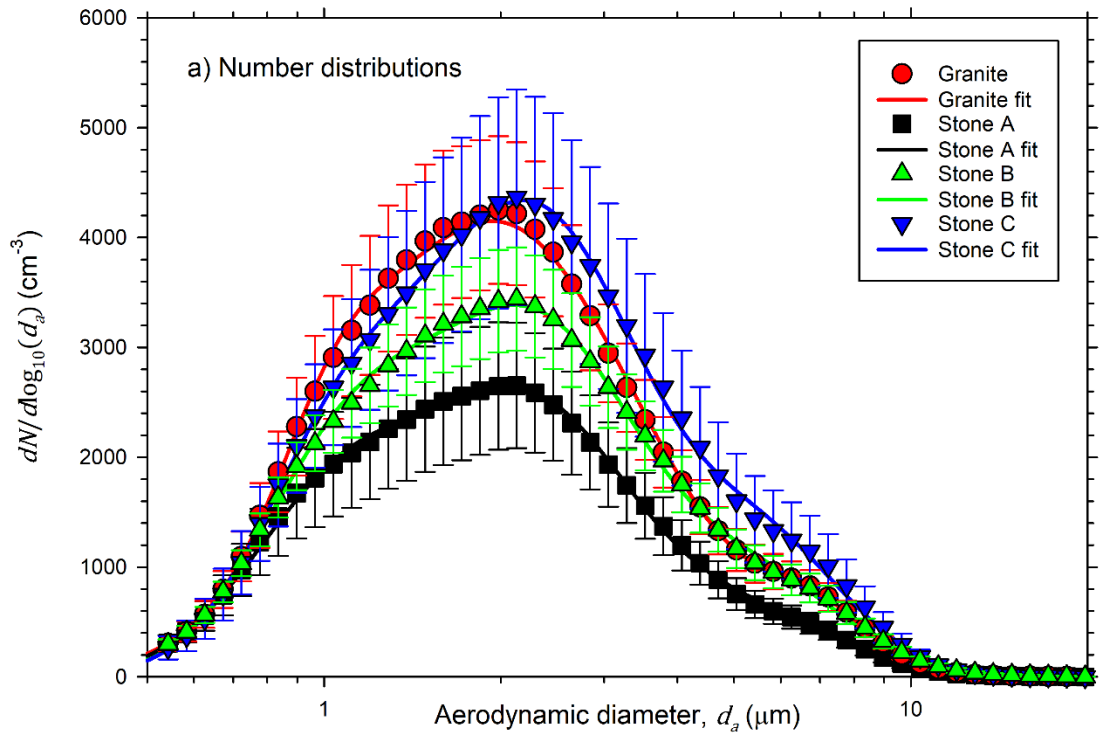


Figure 4. Volume removal rate from three experimental runs of grinding ~30 mm thick samples of Granite and Stones A – C in (a) and ~20 mm thick samples of Stones 1 – 5 in (b). Error bars represent the standard deviation of three replicates.

Particle Size Distributions

The number-based and mass-based particle size distributions measured during stone product grinding by the APS, and corrected to account for particle density and shape, are plotted in Figure 5(a) and (b) for Granite and Stones A through C, and Figure 5(c) and (d) for Stones 1 through 5. Plotted along with the APS data are the best fit trimodal lognormal distributions (see Table 4 in Appendix I for the best fit, number-based, trimodal lognormal distribution parameters). The total number concentration was highest during the grinding of Stone C, followed in decreasing order by Granite, Stone B, Stone A, Stone 4, Stone 1, Stone 2, Stone 3, and Stone 5. In the number-based size distributions, all stone products, excluding Stone 5, had their most prominent mode located at an aerodynamic diameter of about 2.0 – 2.5 μm , second most prominent mode at 0.93 – 1.1 μm , and least prominent mode at 5.1 – 6.9 μm . While this was also true for Stone 5 when looking at absolute concentrations, when considering the relative contribution of the fitted lognormal distributions the most prominent mode was at 4.0 μm , second most at 1.1 μm , and least at 2.2 μm . The trimodal lognormal distributions exhibited an excellent fit with coefficients of determination, R^2 , greater than 0.99 for all stones. Following the methodology outlined in Appendix I to derive mass-based distributions from the best fit number-based size distributions, we see the most prominent modes at 5.1 – 8.0 μm in the mass-based size distributions for all the stone products evaluated in this study, as shown in Figure 5(b) and (d) (see Table 5 in Appendix I for the derived mass-based, trimodal lognormal distribution parameters).



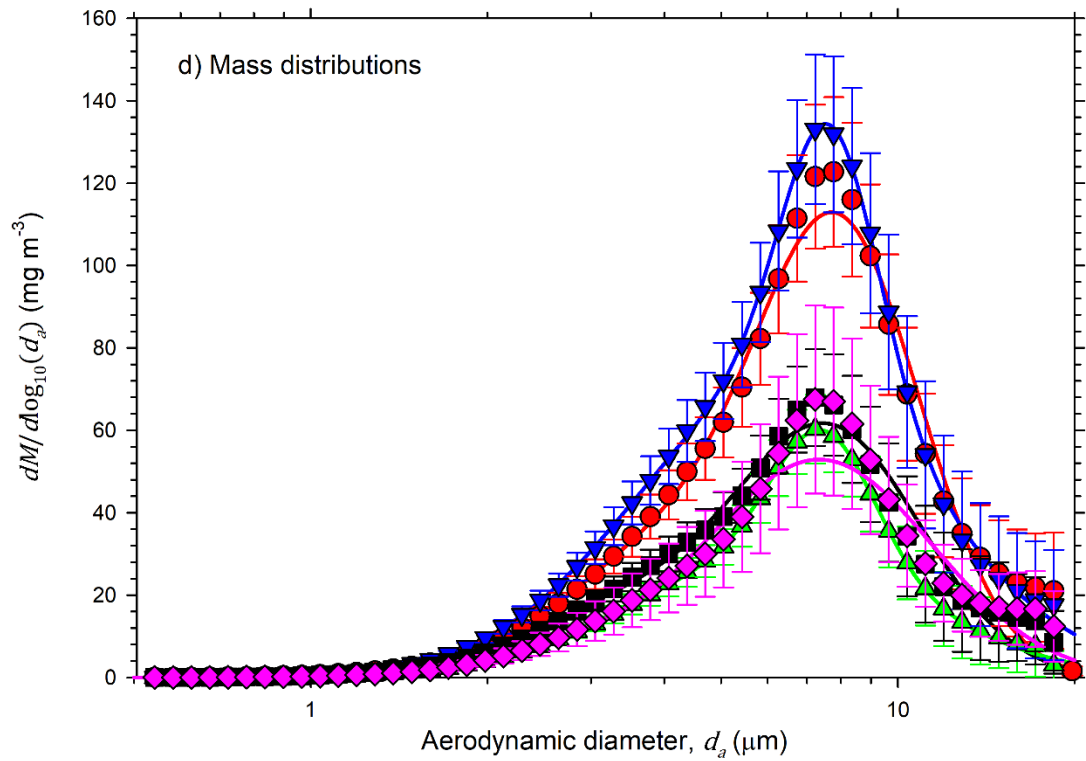
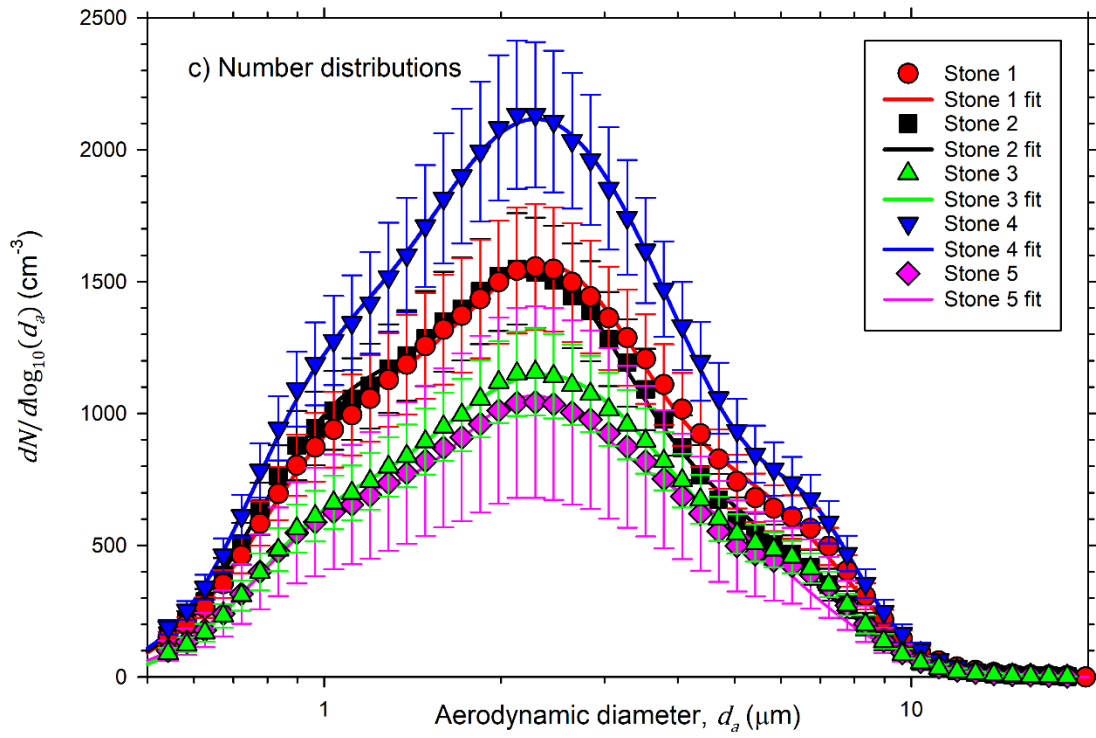


Figure 5. Number-based and mass-based particle size distributions of dust generated during grinding of ~30 mm thick samples of Granite and Stones A – C in (a) and (b) and ~20 mm thick samples of Stones 1 – 5 in (c) and (d). Error bars represent the standard deviation. Curves are best fit trimodal lognormal distributions.

Discussion

Comparison of Crystalline Silica Content

Three recent related studies have characterized the emissions from engineered stone products with a resin matrix and granite, along with sintered artificial stone and other natural stones, in a controlled environment. Carrieri et al. [2020] and Ramkissoon et al. [2022] investigated stone cutting and Hall et al. [2022] investigated stone cutting and polishing. All three previous studies found that the crystalline silica content in dust generated from cutting or polishing of engineered stone products with a resin matrix (37 – 91 wt%) was higher than that for granite (1.9 – 30 wt%). With one exception, the results from the present study were similar. The crystalline silica content of respirable dust generated from the dry grinding of all engineered stone products with a resin matrix surveyed, excluding Stone B, ranged from 57 to 75 wt%. This was markedly higher crystalline silica content than that for the granite stone product (24.5 ± 5.1 wt%). Stone B employed a new formula to lower crystalline silica content and had a crystalline silica content of respirable dust equal to 26.0 ± 2.9 wt%, comparable to that measured for Granite. No crystalline silica was detected in the respirable dust from Stone C which was an engineered stone consisting of recycled glass in a cement matrix. This is lower than the crystalline silica content in respirable dust generated from the grinding, cutting, or polishing of all engineered stone, sintered artificial stone, and natural stone products investigated by Carrieri et al. [2020], Hall et al. [2022], Ramkissoon et al. [2022], and the present study.

Like that seen by Hall et al. [2022] during stone cutting, we observed that the crystalline silica content in respirable dust collected during the grinding of each stone product investigated in this study was equivalent to that in the bulk material/dust samples. In addition, recent studies using cascade impactors have shown that crystalline silica content in the dust generated from stone product fabrication tasks varied little with dust particle size. Hall et al. [2022] reported that the crystalline silica content in dust from the cutting and polishing of engineered stone, sintered artificial stone, and natural stone product collected on each stage of a cascade impactor was consistent with that in the bulk material, except in some cases where the mass collected on the bottom-most stage of the impactor approached the LOQ. Thompson and Qi [2023] found that there was no statistically significant difference in the crystalline silica content in dust from the grinding of engineered stone and granite stone products collected on any cascade impactor stage in comparison with the total dust samples from closed-face cassettes. All of this suggests that crystalline silica content in the bulk dust could be representative of crystalline silica content in the respirable dust generated during grinding.

Comparison of Particle Size Distribution

For the number-based size distributions measured in this study, all stone products, excluding Stone 5, had their most prominent mode located at an aerodynamic diameter of about 2.3 – 2.5 μm , second most prominent mode at 0.93 – 1.1 μm , and least prominent mode at 5.1 – 6.9 μm . For Stone 5, the most prominent mode was at 4.0 μm , second most at 1.1 μm , and least at 2.2 μm . We should note that the fitting procedure accounts for the standard deviation of the data in the optimization. The fact that the relative standard deviations of size distribution data for Stone 5 were, on average, larger than those for the other stone products may explain the differences in the relative contributions of each mode. The mass-based distributions from the same best fit procedure show the most prominent modes at 5.1 – 8.0 μm for all the stone products evaluated in this study. This suggests that the mechanical process of the fabrication task, in this case a pneumatic angle grinder equipped with a coarse diamond grinding cup wheel, rather than the type of stone product predominantly determines the shape of the dust size distribution. It is plausible that different fabrication tasks (e.g., cutting, grinding, and polishing) can lead to airborne dust with varying size distribution shapes. Qualitatively, the number-based size distributions reported here are comparable to the mode measured by Carrieri et al. [2020] in the supermicrometer particle range. The mass-based size distributions found in this study fell between those observed during cutting by Carrieri et al. [2020], with a mode between 3 and 10 μm , and by Hall et al. [2022], with modes at 6 and 9 μm . The mass-based size distributions measured in this study had larger modes than those measured by Hall et al. [2022] during stone polishing, where the major peak was observed at 0.1 μm and another at 2.5 μm .

Comparison of Generation Rate

Using the normalized generation rate as a metric for characterizing the emissions from subtractive processes, such as grinding, sanding, and cutting, enables comparison of emissions from different studies on different tasks and provides valuable input parameters for modeling workplace exposure. Nominal values of concentrations will be dependent on the dilution occurring in the testing system used to generate the data. In contrast, a generation rate obtained by following the European Standard EN 1093-3 is independent of system dilution rates and allow for comparisons between studies. The normalized generation rate, defined in Equation 1, is the mass of emissions generated per unit of volume removed from the workpiece. The nominal generation rate, typically represented in mass per unit of time, was normalized to include the effect of material removed from the corresponding grinding activity (see Figure 4 for the material volume removal rates measured in this study). The volume removed from workpieces by grinding might be estimated from geometric measurements and/or countertop design features, such as dimensions of slabs, dimensions of cutouts, radii of corners, edge profiles, etc. With the normalized generation rate, the RCS mass generated by a worker during the full-shift may be derived, which may then be readily incorporated into a model to estimate the worker's RCS exposure after consideration of aerosol dispersion, background concentration, and other modeling factors. Furthermore, by

comparing the normalized generation rate with and without the use of different engineering control measures, the effectiveness of the control measures can be evaluated. Such an approach will allow prompt identification and optimization of feasible control measures in a standard laboratory setting prior to more expensive field validations as was done by a study from NIOSH [2014] on controlling RCS exposures from cutting fiber-cement.

For identical amounts of materials removed from grinding activities within similar time frames, a worker's time-weighted-average RCS exposure is likely to be commensurate with the normalized generation rate of RCS for a given identical stone product obtained at the same workplace setting. Among the four stone products that were studied with samples that were about 30 mm thick, the three engineered stones (Stone A, B and C) had similar dust generation rates and their RCS generation rates were largely affected by the silica content. It is notable that Stone B, which is a new formula with lower silica content, resulted in an RCS generation rate considerably lower than Stone A and even 42% lower than the granite investigated in this study; and Stone C, which has no crystalline silica in its formula, indeed generated no detectable crystalline silica. Among the five engineered stones that were studied with samples of about 20 mm thick, the silica content (Figure 2), dust and RCS generation rates (Figure 3), as well as volume removal rates (Figure 4), all remain in relatively narrow ranges, suggesting that workers are expected to be exposed to similar levels of RCS when grinding these products at the same workplace setting.

In this same study, we used a cascade impactor as the sampler in the place of the respirable dust sampler and obtained the size-dependent normalized generation rates of RCS for the Granite and Stone A to C. By incorporating the respirable fraction criterion at the midpoint aerodynamic diameter of each stage of the cascade impactor, Thompson and Qi [2023] reported the size-dependent normalized generation rates of RCS for the Granite and Stone A to C. The highest normalized generation rate of RCS consistently occurred at 3.2 – 5.6 μm for all the stones containing crystalline silica. When developing engineering control measures, removing particles in this size range near the generation sources should be prioritized to maximize RCS reduction.

Limitations and Implications of the Experiment Results

While we maintain that normalized generation rate is a useful metric for comparing emissions generated by different materials or tasks, care must be taken when designing studies or interpreting results from separate studies. There may be factors associated with the sample or fabrication task that when not held constant could contribute to differences in the normalized generation rate. For instance, Stone A and Stone 4 are both engineered stone products from the same manufacturer and ostensibly with similar compositions. However, the two samples differed in thickness. The sample for Stone A was 30 mm thick and consisted of 7 substrates stacked and clamped together. The sample for Stone 4 was 19 mm thick and was a single, solid substrate. While the dust emissions were comparable for Stone A and Stone 4 (similarly shaped particle size distributions, number

concentration measured by APS was 20% higher for Stone A than Stone 4, the mass concentration measured by respirable sampler was 7% higher for Stone A than Stone 4, and the crystalline silica content of respirable dust was about 10% lower for Stone A than Stone 4), the volume removal rate for Stone A was 50% of that for Stone 4. This resulted in the normalized generation rates of respirable dust and RCS being about twice as high for Stone A than Stone 4. It is possible that differences in the contact surface area of the grinding cup wheel brought about by the differing sample thickness could account for the large disagreement in volume removal rate and the resulting normalized generation rates. A larger contact area could result in a larger torque acting on the angle grinder. For a pneumatic angle grinder, this increased torque would result in a linear decrease in rotational speed [Beater, 2007]. While a mechanistic investigation of the coupling of contact surface area, material removal rates, and respirable dust emission rates is beyond the scope of this study, one might reasonably presume that the contact surface area of the grinding wheel with the workpiece would influence the material removal rate. For this reason, in the results we address the normalized generation rate and volume removal rate results separately for samples of differing thickness. We must also add that although the angle grinder was operated by the same two individuals throughout this study and they tried to maintain similar grinding performance, it is possible that the force applied, the angle of the grinder, and traverse speed of the grinder varied, especially given the fact that the tests for the ~20 cm and ~30 cm stone products were performed nearly one year apart. Despite the limitations described above, the two groups of experimental results provide valuable comparisons.

Conclusions and Recommendations

During grinding, all stones were found to generate similar trimodal lognormal mass-weighted particle size distributions with the most prominent mode located at an aerodynamic diameter of about 5.1 – 8.0 μm , suggesting that the mechanical process of dust formation from grinding different stones is similar and engineering control measures for the grinding task may be consistently applicable to all stone types. The crystalline silica content in bulk dust was found to be equivalent to that of respirable dust for all stones investigated, suggesting that crystalline silica content in the bulk dust could be representative of that in respirable dust generated during grinding.

Controlling exposures to occupational hazards is the fundamental method of protecting workers. Traditionally, a hierarchy of controls has been used as a means of determining how to implement feasible and effective controls. One representation of the hierarchy controls can be summarized as follows:

- Elimination
- Substitution
- Engineering Controls (e.g., ventilation)
- Administrative Controls (e.g., reduced work schedules)
- Personal Protective Equipment (PPE, e.g., respirators)

The idea behind this hierarchy is that the control methods at the top of the list are potentially more effective, protective, and economical (in the long run) than those at the bottom. Following the hierarchy normally leads to the implementation of inherently safer systems, ones where the risk of illness or injury has been substantially reduced.

Based on the normalized RCS generation rates, with the same amount of grinding activities and control effectiveness, workers are likely to be exposed to similar levels of RCS when working with engineered stones from different manufacturers that have similar thicknesses and colors and contain similarly high levels of silica content (up to about 90 wt%) in a resin matrix. Correspondingly, workers are likely to be exposed to lower concentrations of RCS when working with engineered stones containing no crystalline silica (e.g., Stone C), followed by engineered stones specifically designed with lower silica content (e.g., Stone B), then granite similar to the one in this study, and finally engineered stones that contain high silica content. The manufacturing and adoption of engineered stone products with formulations such as Stone B could potentially lower RCS exposure risks to levels comparable to that associated to working with most natural stones, while adoption of products similar to Stone C may eliminate the risks of RCS exposure completely. This would adhere to the top of the hierarchy of controls and could be effectively incorporated in a layered, overall control strategy. For developing engineering controls within the same overall control strategy, prioritizing the removal of particles in the range of 3.2 – 5.6 μm near the generation sources should help maximize RCS reduction, since the highest normalized generation rate of RCS consistently occurred in this size range for all the stones containing crystalline silica in this study.

References

- 81 Fed. Reg. 16285 [2016]. Occupational Safety and Health Administration: occupational exposure to respirable crystalline silica, final rule. <https://www.federalregister.gov/documents/2016/03/25/2016-04800/occupational-exposure-to-respirable-crystalline-silica>
- Beater P [2007]. Pneumatic Drives: System Design, Modelling and Control. Berlin, Heidelberg: Springer Berlin Heidelberg.
- Blatt H, Tracy R [1997]. Petrology: igneous, sedimentary and metamorphic (2nd ed.). New York, NY: W.H. Freeman and Company. p. 66.
- Branch MA, Coleman TF, Li Y [1999]. A Subspace, Interior, and Conjugate Gradient Method for Large-Scale Bound-Constrained Minimization Problems. SIAM J Sci Comput, 21(1): 1-23.
- Brockmann JE [2011]. Aerosol Transport in Sampling Lines and Inlets. *In*: Kulkarni P, Baron PA, Willeke K Eds. Aerosol measurement : principles, techniques, and applications). Hoboken, NJ: John Wiley & Sons, Inc. p. 69.

Bureau of Mines [1992]. Crystalline Silica Primer. Washington, DC: U.S. Department of the Interior, Bureau of Mines, Branch of Industrial Minerals. Special Publication.

Carrieri M, Guzzardo C, Farcas D, Cena LG [2020]. Characterization of Silica Exposure during Manufacturing of Artificial Stone Countertops. *Int J Environ Res Public Health*, 17(12): 4489.

CEN [2006]. EN 1093-3, Safety of machinery - Evaluation of the emission of airborne hazardous substances - Part 3: Test bench method for the measurement of the emission rate of a given pollutant. Brussels, Belgium: European Committee for Standardization.

Davies CN [1979]. Particle-fluid interaction. *J Aerosol Sci*, 10(5): 477-513.

Fazio JC, Gandhi SA, Flattery J, Heinzerling A, Kamangar N, Afif N, Cummings KJ, Harrison RJ [2023]. Silicosis Among Immigrant Engineered Stone (Quartz) Countertop Fabrication Workers in California. *JAMA Intern Med*, 183(9):991-998.

Friedman GK, Harrison R, Bojes H, Worthington K, Filios M [2015]. Notes from the field: silicosis in a countertop fabricator - Texas, 2014. *Morb Mortal Wkly Rep*, 64(5):129-130.

Glass DC, Dimitriadis C, Hansen J, Hoy RF, Hore-Lacy F, Sim MR [2022]. Silica Exposure Estimates in Artificial Stone Benchtop Fabrication and Adverse Respiratory Outcomes. *Ann Work Expo Health*, 66(1): 5-13.

Hall S, Stacey P, Pengelly I, Stagg S, Saunders J, Hambling S [2022]. Characterizing and Comparing Emissions of Dust, Respirable Crystalline Silica, and Volatile Organic Compounds from Natural and Artificial Stones. *Ann Work Expo Health*, 66(2): 139-149.

Hatch T, Choate SP [1929]. Statistical description of the size properties of non uniform particulate substances. *J Franklin Inst*, 207(3): 369-387.

Hinds WC [1999]. *Aerosol technology: properties, behavior, and measurement of airborne particles*. New York, NY: John Wiley & Sons, Inc.

International Organization for Standardization [2008]. Uncertainty of measurement-Part 3: Guide to the expression of uncertainty in measurement (GUM: 1995). Switzerland: International Organization for Standardization.

Kramer MR, Blanc PD, Fireman E, Amital A, Guber A, Rhahman NA, Shitrit D [2012]. Artificial Stone Silicosis: Disease Resurgence Among Artificial Stone Workers. *Chest*, 142(2): 419-424.

Lofgren DJ [2008]. Results of Inspections in Health Hazard Industries in a Region of the State of Washington. *J Occup Environ Hyg*, 5(6): 367-379.

Marshall IA, Mitchell JP, Griffiths WD [1991]. The behaviour of regular-shaped non-spherical particles in a TSI aerodynamic particle sizer. *J Aerosol Sci*, 22(1): 73-89.

NIOSH [1986]. Occupational respiratory diseases. Cincinnati, OH: U.S. Department of Health and Human Services, Public Health Service, Centers for Disease Control and Prevention, National Institute for Occupational Safety and Health, DHHS (NIOSH) Publication No. 86-102.

NIOSH [1998]. Particles not otherwise regulated, respirable. NIOSH Manual of Analytical Methods (NMAM®), 4th ed., 2nd Supplement, Schlecht PC, O'Connor PF Eds. Cincinnati, OH: U.S. Department of Health and Human Services, Public Health Service, Centers for Disease Control and Prevention, National Institute for Occupational Safety and Health, National Institute for Occupational Safety and Health, DHHS (NIOSH) Publication No. 98-119.

NIOSH [2002]. NIOSH Hazard Review: Health Effects of Occupational Exposure to Respirable Crystalline Silica. Cincinnati, OH: U.S. Department of Health and Human Services, Public Health Service, Centers for Disease Control and Prevention, National Institute for Occupational Safety and Health, DHHS (NIOSH) Publication No. 98-119.

NIOSH [2003]. SILICA, CRYSTALLINE, by XRD (filter redeposition). NIOSH Manual of Analytical Methods (NMAM®), 4th ed., 3rd Supplement, Schlecht PC, O'Connor PF Eds. Cincinnati, OH: U.S. Department of Health and Human Services, Public Health Service,, Centers for Disease Control and Prevention, National Institute for Occupational Safety and Health, DHHS (NIOSH) Publication No. 2003-154.

NIOSH [2014]. Evaluation of the dust generation and engineering control for cutting fiber-cement siding. By Qi C, Echt A, Gressel M, Feng HA. Cincinnati, OH: U.S. Department of Health and Human Services, Centers for Disease Control and Prevention, National Institute for Occupational Safety and Health, EPHB Report No. 358-16a. <https://www.cdc.gov/niosh/surveyreports/pdfs/358-16a.pdf>

NIOSH [2016a]. Evaluation of Crystalline Silica Exposure during Fabrication of Natural and Engineered Stone Countertops. By Zwack LM, Victory KR, Brueck SE, Qi C. Cincinnati, OH: U.S. Department of Health and Human Services, Centers for Disease Control and Prevention, National Institute for Occupational Safety and Health, HHE Report No. 2014-0215-3250. <https://www.cdc.gov/niosh/hhe/reports/pdfs/2014-0215-3250.pdf>

NIOSH [2016b]. Engineering Control of Silica Dust from Stone Countertop Fabrication and Installation, In-depth field survey report for the Houston, TX field survey. By Qi C, Echt A. Cincinnati, OH: U.S. Department of Health and Human Services, Centers for Disease Control and Prevention, National Institute for Occupational Safety and Health, EPHB Report NO. 375-11a. <https://www.cdc.gov/niosh/surveyreports/pdfs/375-11a.pdf>

NIOSH [2016c]. Engineering Control of Silica Dust from Stone Countertop Fabrication and Installation, In-depth field survey report for the Mendota Heights,

MN field survey. By Qi C, Lo L. Cincinnati, OH: Department of Health and Human Services, Centers for Disease Control and Prevention, National Institute for Occupational Safety and Health, EPHB Report No. 375-12a.

<https://www.cdc.gov/niosh/surveyreports/pdfs/375-12a.pdf>

NIOSH [2021]. Engineering Control of Silica Dust from Stone Countertop Fabrication and Installation – Evaluation of Wetting Methods for Grinding. By Qi C, Echt A. Cincinnati, OH: U.S. Department of Health and Human Services, Centers for Disease Control and Prevention, National Institute for Occupational Safety and Health, EPHB Report NO. 2021-DFSE-710.

<https://www.cdc.gov/niosh/surveyreports/pdfs/2021-DFSE-710.pdf>

NIOSH, OSHA [2015]. Worker exposure to silica during countertop manufacturing, finishing and installation. National Institute for Occupational Safety and Health, Occupational Safety and Health Administration, DHHS (NIOSH) Publication No. 2015-106, OSHA HA-3768-2015.

<https://www.osha.gov/sites/default/files/publications/OSHA3768.pdf>

Pérez-Alonso A, Córdoba-Doña JA, Millares-Lorenzo JL, Figueroa-Murillo E, García-Vadillo C, Romero-Morillo J [2014]. Outbreak of silicosis in Spanish quartz conglomerate workers. *Int J Occup Environ Health*, 20(1): 26-32.

Phillips ML, Johnson AC [2012]. Prevalence of Dry Methods in Granite Countertop Fabrication in Oklahoma. *J Occup Environ Hyg*, 9(7): 437-442.

Phillips ML, Johnson DL, Johnson AC [2013]. Determinants of Respirable Silica Exposure in Stone Countertop Fabrication: A Preliminary Study. *J Occup Environ Hyg*, 10(7): 368-373.

Qi C, Echt A, Gressel MG [2016]. On the Characterization of the Generation Rate and Size-Dependent Crystalline Silica Content of the Dust from Cutting Fiber Cement Siding. *Ann Occup Hyg*, 60(2): 220-30.

Qi C, Thompson D, Amy Feng H [2022]. Caution on Using Tetrahydrofuran for Processing Crystalline Silica Samples From Engineered Stone for XRD Analysis. *Ann Work Expo Health*, 66(9): 1210-1214.

Ramkissoon C, Gaskin S, Thredgold L, Hall T, Rowett S, Gun R [2022]. Characterisation of dust emissions from machined engineered stones to understand the hazard for accelerated silicosis. *Sci Rep*, 12(1): 4351.

Rose C, Heinzerling A, Patel K, et al [2019]. Severe silicosis in engineered stone fabrication workers - California, Colorado, Texas, and Washington, 2017-2019. *Morb Mortal Wkly Rep*, 68(38): 813-818.

Seinfeld JH, Pandis SN [2016]. Atmospheric chemistry and physics: from air pollution to climate change. John Wiley & Sons. p. 333.

Thompson D, Qi C [2023]. Characterization of the Emissions and Crystalline Silica Content of Airborne Dust Generated from Grinding Natural and Engineered Stones. *Ann Work Expo Health*, 67(2): 266-280.

TSI Incorporated [2013]. Aerosol Instrument Manager® Software for Aerodynamic Particle Sizer® (APS™) Spectrometers, P/N 1930064, REVISION H.

Vincent JH [2007]. *Aerosol sampling : science, standards, instrumentation and applications*. Chichester, England: John Wiley & Sons Ltd. p. 273.

Virtanen P, Gommers R, Oliphant TE, et al. [2020]. SciPy 1.0: fundamental algorithms for scientific computing in Python. *Nat Methods*, 17(3): 261-272.

Wang H-C, John W [1987]. Particle Density Correction for the Aerodynamic Particle Sizer. *Aerosol Sci Technol*, 6(2): 191-198.

Appendices

Appendix I. Treatment of APS Data

The particle shape and density correction for the APS outlined by Marshall et al. [1991] is identical to the density correction algorithm that is implemented into AIM [Wang and John, 1987] if the particle density, ρ_p , is replaced by the particle density divided by the dynamic shape factor, ρ_p/χ . In this study, particle density and dynamic shape factor were assumed to be particle size-independent and particle density was assumed to be equal to the bulk material density of the stone samples.

Particle dynamic shape factor was unknown and found in the following manner. The mass in APS channel i at time t , $m_{i,t}$, was found using Equation 3 where $n_{i,t}$ is the particle count in channel i at time t and d_{v_i} is the particle volume diameter at the midpoint of channel i .

$$m_{i,t} = \frac{\pi}{6} \rho_p n_{i,t} d_{v_i}^3 \quad \text{Equation 3}$$

Particle volume diameter was related to the particle aerodynamic diameter, d_a , by Equation 4 where ρ_0 is a standard density of 1000 kg m⁻³ [Hinds, 1999].

$$d_v = d_a \sqrt{\chi \frac{\rho_0}{\rho_p}} \quad \text{Equation 4}$$

The respirable mass sampled by the APS, $m_{APS,respir}$, was then found by Equation 5 where R_i is the ACGIH criterion for the respirable fraction [Vincent, 2007] calculated at the midpoint of channel i .

$$m_{APS,respir} = \sum_t \sum_i R_i m_{i,t} \quad \text{Equation 5}$$

The sum of the squared residuals, S , was then determined using Equation 6 where \bar{m}_{sampl_j} is the average respirable mass collected by the respirable samplers in experiment run j , Q_{sampl} is the flowrate of the respirable sampler (9.0 l min⁻¹), and Q_{APS} is the aerosol sample flowrate in the APS (1.0 l min⁻¹).

$$S = \sum_{j=1}^3 \left(\bar{m}_{sampl_j} - \frac{Q_{sampl}}{Q_{APS}} m_{APS,respir_j} \right)^2 \quad \text{Equation 6}$$

The estimated dynamic shape factor was then identified by minimizing the sum of the squared residuals as demonstrated in Figure 6. The best fit dynamic shape factors are listed in Table 4 and ranged from 1.2 to 1.7. These values were comparable to those found by Davies [1979] for quartz (1.36) and sand (1.57).

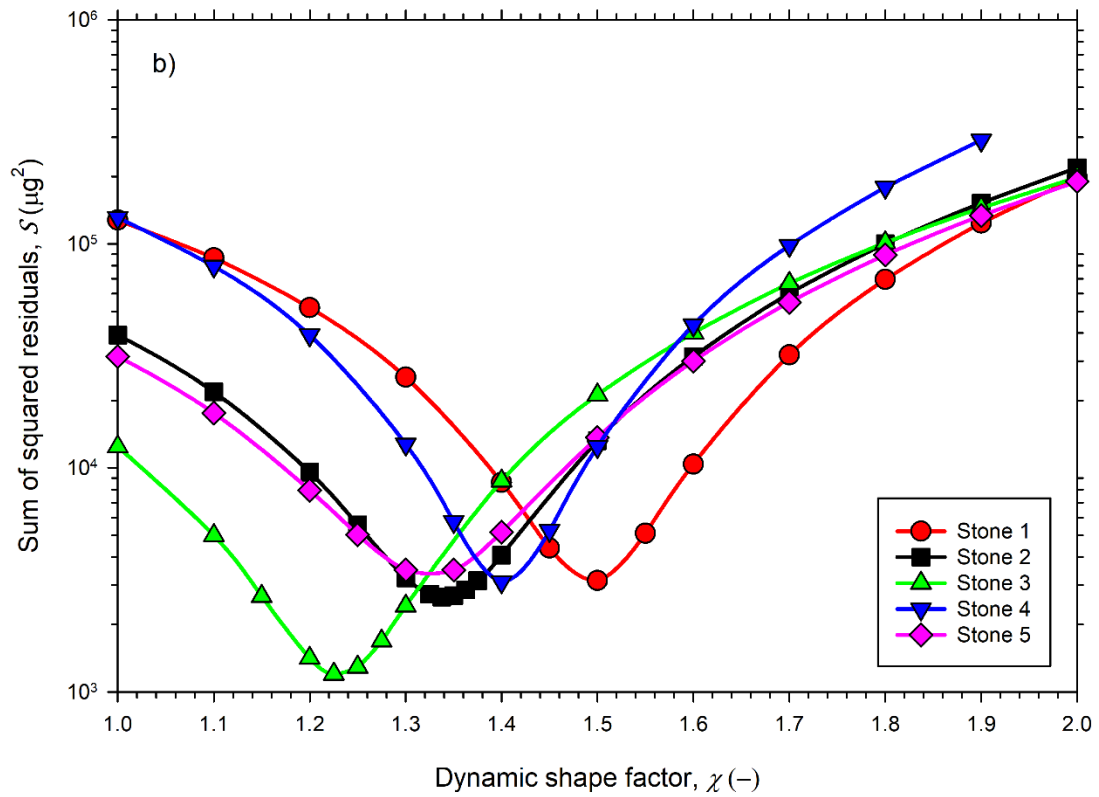
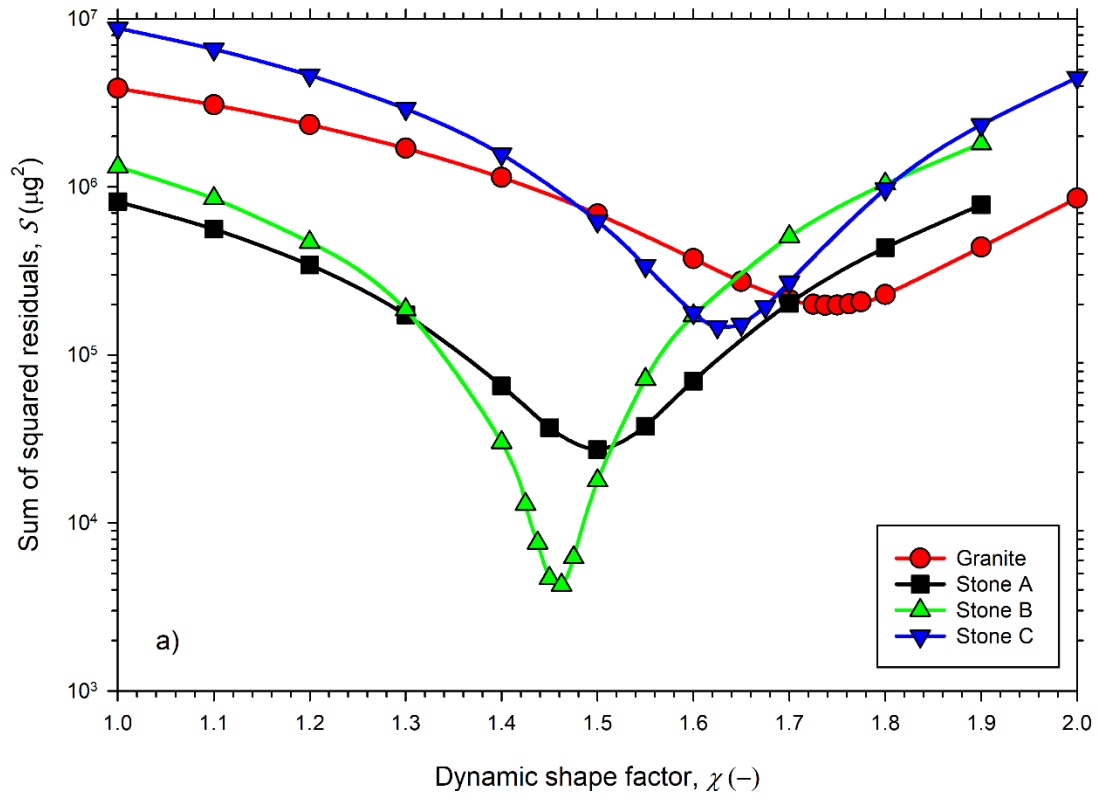


Figure 6. Sum of squared residuals from APS-derived respirable mass as a function of particle dynamic shape factor for a) Granite and Stones A – C and b) Stones 1 – 5. Plotted curves are simple spline curves generated by SigmaPlot (v14.5, Inpixon, USA).

After correcting for particle shape and density, the particle number distribution measurements, $dN/d \log_{10}(d_a)$, were averaged over the periods of active grinding from the three experimental runs. Particle size distributions expressed as a function on the common logarithm of the particle diameter were related to size distributions as a function of the natural logarithm of particle diameter by $dN/d \log_{10}(d_a) = \ln(10) dN/d \ln(d_a)$ [Seinfeld and Pandis, 2016]. Number-based, trimodal lognormal size distribution functions, as defined in Equation 7, were then fit to the APS-measured number-based particle size distributions and standard deviations using the Trust Region Reflective minimization algorithm [Branch et al., 1999] implemented in the Python package SciPy [Virtanen et al., 2020]. Here, N_i is the number concentration of mode i , CMD_i is the count median aerodynamic diameter of mode i , and σ_{g_i} is the geometric standard deviation of mode i .

$$f_N(\ln d_a) = \sum_{i=1}^3 \frac{N_i}{\sqrt{2\pi} \ln \sigma_{g_i}} \exp \left[-\frac{(\ln d_a - \ln CMD_i)^2}{2 (\ln \sigma_{g_i})^2} \right] \quad \text{Equation 7}$$

Parameters for the best fit distribution are summarized in Table 4. For convenience, the total number concentration, $N_T = \sum_{i=1}^3 N_i$, was factored out of the results to allow for easier comparisons of the weight of each mode, $w_{N_i} = N_i/N_T$, when reporting results.

Table 4. Best fit dynamic shape factor and number-based, trimodal lognormal distribution parameters (and resulting coefficient of determination, R^2) for particle size distributions measured by APS

Stone	χ (-)	N_T (cm^{-3})	w_{N_1} (-)	CMD_1 (μm)	σ_{g_1} (-)	w_{N_2} (-)	CMD_2 (μm)	σ_{g_2} (-)	w_{N_3} (-)	CMD_3 (μm)	σ_{g_3} (-)	R^2 (-)
Granite	1.7	2830	0.0701	1.03	1.25	0.893	1.96	1.75	0.0373	6.88	1.24	1.0
A	1.5	1860	0.374	1.09	1.45	0.525	2.32	1.47	0.101	5.44	1.41	1.0
B	1.5	2420	0.328	1.11	1.43	0.550	2.34	1.49	0.122	5.59	1.41	1.0
C	1.6	2990	0.240	1.08	1.40	0.643	2.31	1.53	0.117	5.81	1.37	1.0
1	1.5	1160	0.279	1.08	1.45	0.571	2.48	1.51	0.150	5.87	1.38	1.0
2	1.3	1110	0.330	1.08	1.44	0.497	2.35	1.44	0.174	5.08	1.44	1.0
3	1.2	838	0.106	0.939	1.33	0.842	2.37	1.76	0.0524	6.64	1.22	1.0
4	1.4	1550	0.0942	0.926	1.32	0.867	2.30	1.79	0.0385	6.88	1.21	1.0
5	1.3	776	0.341	1.14	1.47	0.269	2.22	1.33	0.391	4.03	1.56	0.99

A mass-based, trimodal lognormal size distribution, as shown in Equation 8, was then derived from these best fit parameters. Here, M_i is the mass concentration of mode i and MMD_i is the mass median aerodynamic diameter of mode i .

$$f_M(\ln d_a) = \sum_{i=1}^3 \frac{M_i}{\sqrt{2\pi} \ln \sigma_{g_i}} \exp \left[-\frac{(\ln d_a - \ln MMD_i)^2}{2 (\ln \sigma_{g_i})^2} \right] \quad \text{Equation 8}$$

Equation 9 was used to calculate M_i where $d_{\bar{m}_i}$ is the particle diameter of average mass of mode i .

$$M_i = \frac{\pi}{6} \rho_p d_{\bar{m}_i}^3 N_i \quad \text{Equation 9}$$

The diameters of average mass and mass median diameters were found using the Hatch-Choate equations [Hatch and Choate, 1929; Hinds, 1999] in Equation 10 and Equation 11, respectively, where CMD_{v_i} is the count median volume diameter of mode i . The count median aerodynamic diameter and count median volume diameter were related using Equation 4.

$$d_{\bar{m}_i} = CMD_{v_i} \exp \left[\frac{3}{2} (\ln \sigma_{g_i})^2 \right] \quad \text{Equation 10}$$

$$MMD_i = CMD_i \exp \left[3 (\ln \sigma_{g_i})^2 \right] \quad \text{Equation 11}$$

The derived, mass-based, trimodal lognormal distribution parameters are summarized in Table 5. Again, the total mass concentration, $M_T = \sum_{i=1}^3 M_i$, was factored out of the results to allow for easier comparisons of the weight of each mode, $w_{M_i} = M_i/M_T$, when reporting results.

Table 5. Derived, mass-based, trimodal lognormal distribution parameters (and resulting coefficient of determination, R^2) for particle size distributions measured by APS

Stone	M_T (mg m ⁻³)	w_{M_1} (-)	MMD_1 (μm)	w_{M_2} (-)	MMD_2 (μm)	w_{M_3} (-)	MMD_3 (μm)	R^2 (-)
Granite	94.3	0.00225	1.20	0.646	5.06	0.351	7.91	0.99
A	48.8	0.0218	1.64	0.309	3.59	0.669	7.71	0.98
B	79.0	0.0155	1.64	0.280	3.74	0.704	7.97	0.98
C	119	0.00928	1.51	0.330	3.97	0.661	7.82	0.99
1	50.9	0.00968	1.63	0.276	4.12	0.714	8.00	0.98
2	30.9	0.0142	1.62	0.215	3.48	0.771	7.62	0.98
3	25.0	0.00193	1.20	0.719	6.19	0.279	7.48	1.0
4	59.1	0.00167	1.17	0.767	6.39	0.232	7.67	1.0
5	27.7	0.0144	1.77	0.0625	2.84	0.923	7.35	0.95

Appendix II. Additional Tables and Figures

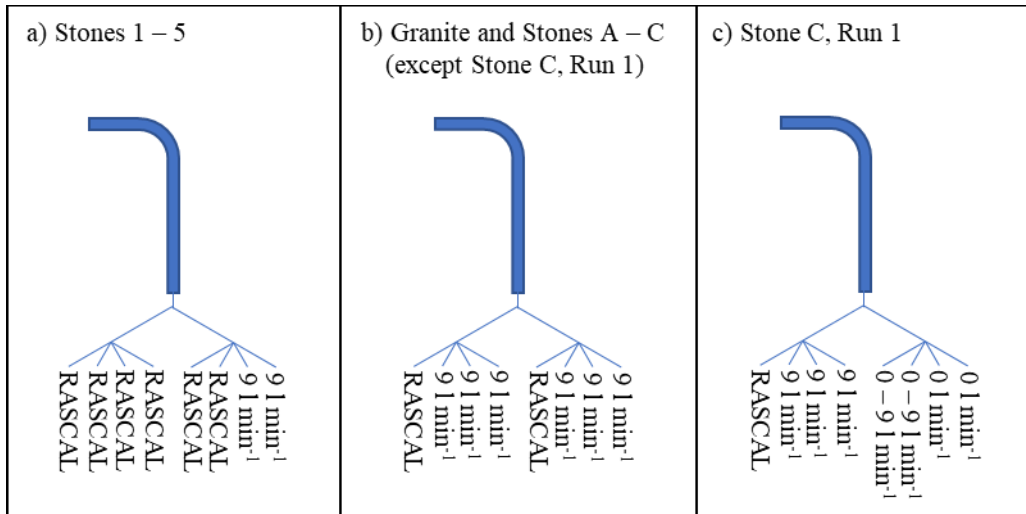


Figure 7. Differing sampling train configurations for respirable samplers (RASCALs) for each stone/experimental run. Note that in (c) two ports of a 4-way flow splitter show flow rates of 0 - 9 l min⁻¹. This is because two pumps collecting samples unrelated to this study malfunctioned and turned off mid-run.

Appendix III. Tabulated Data from Figures

Table 6. Crystalline silica content of respirable dust

Stone	Cristobalite (wt%)		Quartz (wt%)		Crystalline silica (wt%)	
	Average	Combined standard uncertainty	Average	Combined standard uncertainty	Average	Combined standard uncertainty
Granite	0.0	0.0	24.6	5.1	24.6	5.1
A	41.6	9.6	15.8	5.0	57	13
B	17.0	2.3	9.1	1.1	26.0	2.9
C	0.0	0.0	0.0	0.0	0.0	0.0
1	41	11	19.8	5.3	61	14
2	12.5	2.5	61	15	73	16
3	0.0	0.0	75	15	75	15
4	42.3	6.5	23.1	3.5	65.4	8.3
5	46	11	15.0	3.8	61	13

Table 7. Normalized generation rates

Stone	RCS (mg cm ⁻³)		Respirable dust (mg cm ⁻³)	
	Average	Combined standard uncertainty	Average	Combined standard uncertainty
Granite	10.8	2.9	43.4	9.4
A	15.6	1.5	27.4	3.6
B	6.31	0.17	24.3	1
C	0	0	25.1	4.3
1	7.5	1.1	12.3	1.5
2	7.2	1.2	9.9	1.6
3	5.7	1.0	7.6	1.0
4	8.4	1.2	12.8	1.4
5	5.57	0.79	9.2	1.3

Table 8. Volume removal rates

Stone	Average (cm ³ min ⁻¹)	Standard deviation (cm ³ min ⁻¹)
Granite	6.0	1.1
A	5.22	0.50
B	8.15	0.96
C	10.0	2.4
1	8.93	0.28
2	8.15	0.61
3	7.86	0.41
4	10.56	0.48
5	7.95	0.52

Table 9. Particle number size distributions from APS

Midpoint aerodynamic diameter, d_a (μm)	$dN/d\log_{10}(d_a)$ (cm^{-3})							
	Granite		Stone A		Stone B		Stone C	
	Avg	StDev	Avg	StDev	Avg	StDev	Avg	StDev
0.542	305	67	307	75	300	42	270	110
0.583	414	90	410	100	410	54	370	140
0.626	570	120	550	130	564	72	530	180
0.673	800	170	740	180	775	94	750	240
0.723	1100	230	970	240	1030	120	1040	290
0.777	1470	290	1230	300	1340	150	1390	340
0.835	1870	370	1460	360	1630	180	1750	380
0.898	2280	450	1670	410	1920	220	2100	430
0.965	2600	510	1810	450	2130	250	2380	470
1.037	2910	560	1940	480	2330	290	2640	530
1.114	3150	600	2040	500	2490	310	2860	580
1.197	3380	630	2140	520	2650	340	3070	640
1.286	3630	670	2260	540	2830	370	3310	700
1.382	3800	680	2340	560	2970	400	3490	750
1.486	3970	700	2440	570	3110	420	3700	800
1.596	4090	700	2510	580	3210	440	3880	850
1.715	4140	690	2560	580	3280	450	4030	880
1.843	4200	680	2600	580	3350	460	4180	920
1.981	4250	670	2650	580	3420	470	4320	960
2.129	4220	650	2650	570	3440	470	4370	980
2.288	4070	620	2590	540	3370	460	4300	980
2.458	3870	580	2480	510	3260	450	4170	960
2.642	3570	540	2310	470	3070	430	3960	930
2.839	3290	500	2140	430	2870	400	3750	900
3.051	2950	450	1930	380	2640	370	3470	840
3.278	2630	400	1740	340	2410	340	3200	790
3.523	2340	360	1560	300	2190	310	2930	740
3.786	2050	320	1370	260	1970	280	2640	680
4.068	1780	280	1200	230	1750	250	2360	610
4.371	1550	250	1040	200	1540	230	2090	550
4.698	1330	220	880	170	1340	200	1830	490
5.048	1160	190	750	140	1170	180	1600	430
5.425	1030	170	660	120	1040	160	1440	390
5.829	960	160	600	110	950	150	1330	370
6.264	900	150	550	110	890	140	1240	350
6.732	830	140	489	96	810	130	1140	330
7.234	730	130	420	85	710	120	1010	290
7.774	590	110	337	71	580	100	830	240
8.354	445	84	254	58	447	84	630	190
8.977	313	62	178	47	324	66	450	140
9.647	203	44	119	37	223	51	297	98
10.37	122	31	76	29	146	39	183	65
11.14	72	22	47	22	94	30	109	43
11.97	40	16	29	17	59	22	64	29
12.86	23	12	19	13	37	17	38	20
13.82	14.1	9.3	12.0	9.8	24	12	23	14
14.86	8.6	6.7	8.0	7.2	15.8	9.1	15	11
15.96	5.8	5.7	5.4	5.0	10.5	7.1	10.2	8.9
17.15	3.9	4.4	3.8	4.2	7.2	5.1	7.1	7.2
18.43	2.5	3.4	2.8	3.3	5.2	4.0	5.2	6.1

19.81	-	-	0.52	0.66	0.95	0.83	0.60	0.73
-------	---	---	------	------	------	------	------	------

Midpoint aerodynamic diameter, d_a (μm)	$dN/d\log_{10}(d_a)$ (cm^{-3})									
	Stone 1		Stone 2		Stone 3		Stone 4		Stone 5	
	Avg	StDev	Avg	StDev	Avg	StDev	Avg	StDev	Avg	StDev
0.542	148	24	160	28	90	20	190	27	101	38
0.583	198	30	214	37	124	26	253	36	134	49
0.626	265	39	286	48	168	34	341	47	179	65
0.673	354	52	387	64	233	45	463	63	241	87
0.723	462	68	506	79	310	57	612	81	320	110
0.777	583	84	639	99	398	70	780	100	400	140
0.835	700	100	760	120	483	82	940	120	480	170
0.898	800	120	880	130	563	92	1090	140	550	190
0.965	870	130	940	140	610	96	1190	160	590	210
1.037	940	140	1010	150	660	100	1280	170	630	220
1.114	990	150	1050	160	700	100	1340	180	660	230
1.197	1060	160	1100	160	740	110	1420	190	690	240
1.286	1130	180	1170	170	800	110	1520	210	740	260
1.382	1190	190	1220	170	840	120	1600	220	770	270
1.486	1260	200	1280	180	900	130	1710	230	820	280
1.596	1320	210	1350	190	950	130	1820	250	870	300
1.715	1370	220	1400	200	990	140	1900	260	910	320
1.843	1430	230	1460	200	1060	150	1990	260	960	330
1.981	1500	230	1520	210	1120	150	2080	280	1010	350
2.129	1540	240	1550	210	1150	160	2130	280	1040	360
2.288	1560	240	1530	210	1160	160	2130	280	1040	360
2.458	1550	240	1510	210	1140	160	2110	270	1040	360
2.642	1500	220	1450	200	1110	150	2030	260	1000	350
2.839	1440	210	1390	190	1070	140	1960	250	980	340
3.051	1360	200	1280	180	1020	140	1850	230	920	320
3.278	1290	180	1190	170	960	130	1740	220	870	310
3.523	1210	170	1090	150	900	120	1620	200	820	290
3.786	1110	150	980	140	820	110	1470	180	750	260
4.068	1020	140	870	120	750	100	1330	170	690	240
4.371	920	130	770	110	673	93	1200	150	620	220
4.698	830	110	674	97	601	83	1060	130	550	190
5.048	740	100	594	88	544	75	940	120	500	170
5.425	680	92	540	81	508	70	850	110	470	160
5.829	640	87	502	77	483	66	790	100	440	150
6.264	607	83	466	72	455	61	737	98	420	140
6.732	564	78	416	67	413	56	676	91	390	130
7.234	496	71	351	61	351	48	588	80	340	120
7.774	403	60	275	51	275	41	469	67	272	93
8.354	307	49	202	44	200	34	356	54	202	68
8.977	218	37	140	38	136	28	249	45	139	48
9.647	147	29	92	31	87	21	165	35	92	32
10.37	95	22	60	26	55	17	104	28	59	21
11.14	61	16	39	20	35	14	65	22	38	14
11.97	38	12	25	15	21	12	41	16	26	10
12.86	25.3	9.8	17	11	13.9	9.1	26	13	18.0	7.9
13.82	17.0	7.5	12.5	9.3	9.5	6.8	17.3	9.5	13.0	5.9
14.86	11.9	6.0	9.4	7.2	6.5	5.0	12.2	7.7	9.9	4.7
15.96	8.7	4.9	7.0	5.1	4.4	3.8	8.6	5.8	7.9	4.1
17.15	6.7	4.0	5.3	4.1	3.4	3.3	6.3	4.7	6.3	3.5
18.43	5.2	3.5	2.7	2.4	1.1	1.2	4.7	3.6	3.8	2.6
19.81	0.3	0.2	-	-	-	-	-	-	-	-

Table 10. Particle mass size distributions from APS

Midpoint aerodynamic diameter, d_a (μm)	$dM/d\log_{10}(d_a)$ (mg m^{-3})							
	Granite		Stone A		Stone B		Stone C	
	Avg	StDev	Avg	StDev	Avg	StDev	Avg	StDev
0.542	0.0349	0.0077	0.0324	0.0079	0.0317	0.0044	0.030	0.012
0.583	0.059	0.013	0.054	0.013	0.0539	0.0071	0.052	0.019
0.626	0.101	0.022	0.090	0.022	0.092	0.012	0.090	0.031
0.673	0.175	0.037	0.150	0.037	0.157	0.019	0.160	0.050
0.723	0.298	0.061	0.244	0.060	0.260	0.030	0.275	0.076
0.777	0.497	0.099	0.383	0.094	0.417	0.046	0.46	0.11
0.835	0.78	0.15	0.56	0.14	0.631	0.070	0.71	0.15
0.898	1.19	0.23	0.80	0.20	0.92	0.10	1.06	0.22
0.965	1.68	0.33	1.08	0.27	1.27	0.15	1.49	0.30
1.037	2.34	0.45	1.43	0.35	1.72	0.21	2.05	0.41
1.114	3.14	0.60	1.87	0.46	2.29	0.29	2.76	0.56
1.197	4.18	0.78	2.44	0.59	3.02	0.39	3.68	0.76
1.286	5.6	1.0	3.19	0.77	4.00	0.53	4.9	1.0
1.382	7.2	1.3	4.11	0.98	5.20	0.70	6.4	1.4
1.486	9.4	1.6	5.3	1.2	6.77	0.92	8.5	1.8
1.596	12.0	2.1	6.8	1.6	8.7	1.2	11.0	2.4
1.715	15.0	2.5	8.6	2.0	11.0	1.5	14.2	3.1
1.843	18.9	3.1	10.8	2.4	13.9	1.9	18.3	4.0
1.981	23.8	3.8	13.7	3.0	17.7	2.4	23.4	5.2
2.129	29.3	4.5	17.0	3.7	22.0	3.0	29.4	6.6
2.288	35.1	5.3	20.6	4.3	26.8	3.7	36.0	8.2
2.458	41.3	6.2	24.4	5.0	32.1	4.4	43	10
2.642	47.5	7.2	28.3	5.8	37.5	5.2	51	12
2.839	54.2	8.2	32.4	6.5	43.6	6.1	60	14
3.051	60.2	9.1	36.4	7.2	49.7	7.0	69	17
3.278	67	10	40.7	8.0	56.4	8.0	79	20
3.523	74	11	45.2	8.7	63.7	9.1	89	23
3.786	80	12	49.4	9.5	71	10	100	26
4.068	86	14	54	10	78	11	111	29
4.371	93	15	57	11	85	13	122	32
4.698	99	16	61	12	92	14	132	36
5.048	107	18	64	12	100	15	144	39
5.425	119	20	70	13	110	17	160	44
5.829	137	23	79	15	126	19	184	51
6.264	159	27	89	17	144	23	213	60
6.732	182	32	99	19	164	27	243	69
7.234	198	35	106	21	179	30	267	77
7.774	199	36	105	22	181	32	271	80
8.354	187	35	98	23	173	32	258	77
8.977	163	32	86	22	156	32	227	71
9.647	131	28	71	22	133	30	186	62
10.37	98	25	56	22	108	29	143	51
11.14	71	22	43	20	86	27	106	42
11.97	50	20	33	20	67	26	77	35
12.86	35	19	26	18	52	24	57	29
13.82	27	18	21	17	42	21	43	26
14.86	20	16	17	16	34	20	34	25
15.96	17	17	14	13	28	19	29	25
17.15	14	16	13	14	24	17	25	25
18.43	11	15	12	14	22	17	23	26

19.81	-	-	2.7	3.4	4.9	4.3	3.3	4.0
-------	---	---	-----	-----	-----	-----	-----	-----

Midpoint aerodynamic diameter, d_a (μm)	$dM/d\log_{10}(d_a)$ (mg m^{-3})									
	Stone 1		Stone 2		Stone 3		Stone 4		Stone 5	
	Avg	StDev	Avg	StDev	Avg	StDev	Avg	StDev	Avg	StDev
0.542	0.0153	0.0025	0.0130	0.0023	0.0065	0.0014	0.0181	0.0026	0.0084	0.0032
0.583	0.0254	0.0039	0.0217	0.0037	0.0111	0.0024	0.0301	0.0042	0.0139	0.0051
0.626	0.0421	0.0063	0.0360	0.0060	0.0187	0.0038	0.0500	0.0069	0.0230	0.0084
0.673	0.070	0.010	0.0605	0.0099	0.0322	0.0062	0.085	0.011	0.038	0.014
0.723	0.113	0.017	0.098	0.015	0.0531	0.0098	0.138	0.018	0.062	0.022
0.777	0.177	0.026	0.153	0.024	0.085	0.015	0.220	0.029	0.098	0.035
0.835	0.263	0.038	0.227	0.035	0.127	0.022	0.329	0.042	0.145	0.051
0.898	0.377	0.055	0.326	0.049	0.185	0.030	0.474	0.061	0.207	0.073
0.965	0.508	0.076	0.434	0.064	0.249	0.039	0.639	0.084	0.277	0.097
1.037	0.68	0.10	0.577	0.085	0.335	0.051	0.85	0.11	0.37	0.13
1.114	0.89	0.14	0.75	0.11	0.438	0.065	1.11	0.15	0.47	0.16
1.197	1.17	0.18	0.97	0.14	0.578	0.084	1.46	0.20	0.62	0.22
1.286	1.55	0.24	1.27	0.18	0.77	0.11	1.93	0.26	0.82	0.29
1.382	2.03	0.32	1.65	0.23	1.00	0.14	2.53	0.34	1.07	0.37
1.486	2.67	0.43	2.16	0.30	1.33	0.19	3.36	0.45	1.41	0.49
1.596	3.48	0.55	2.81	0.39	1.75	0.24	4.42	0.60	1.85	0.64
1.715	4.49	0.71	3.61	0.50	2.27	0.31	5.74	0.77	2.40	0.84
1.843	5.82	0.91	4.69	0.64	3.00	0.42	7.47	0.99	3.1	1.1
1.981	7.6	1.2	6.06	0.83	3.95	0.54	9.7	1.3	4.1	1.4
2.129	9.6	1.5	7.6	1.0	5.04	0.70	12.3	1.6	5.3	1.8
2.288	12.1	1.9	9.4	1.3	6.29	0.90	15.3	2.0	6.5	2.3
2.458	14.9	2.3	11.5	1.6	7.7	1.1	18.7	2.4	8.1	2.8
2.642	17.9	2.7	13.6	1.9	9.3	1.3	22.5	2.8	9.7	3.4
2.839	21.4	3.2	16.3	2.2	11.2	1.5	26.9	3.4	11.7	4.1
3.051	25.1	3.6	18.6	2.6	13.1	1.8	31.5	3.9	13.7	4.8
3.278	29.4	4.2	21.5	3.0	15.3	2.1	36.8	4.6	16.1	5.6
3.523	34.2	4.8	24.4	3.4	17.8	2.5	42.4	5.2	18.7	6.5
3.786	39.0	5.4	27.2	3.8	20.2	2.7	47.8	5.9	21.3	7.4
4.068	44.3	6.0	30.0	4.2	22.8	3.1	53.7	6.7	24.2	8.4
4.371	49.9	6.8	32.9	4.7	25.5	3.5	59.9	7.5	27.1	9.5
4.698	55.6	7.6	35.8	5.1	28.3	3.9	65.7	8.3	30	10
5.048	61.9	8.5	39.1	5.8	31.8	4.4	72.0	9.2	34	12
5.425	70.4	9.6	44.1	6.6	36.8	5.1	81	10	39	13
5.829	82	11	50.9	7.8	43.4	5.9	93	12	46	16
6.264	97	13	58.6	9.1	50.8	6.8	108	14	54	19
6.732	111	15	65	10	57.2	7.8	124	17	62	21
7.234	122	17	68	12	60.3	8.3	133	18	68	23
7.774	123	18	66	12	58.5	8.7	132	19	67	23
8.354	116	19	60	13	52.9	8.9	124	19	62	21
8.977	102	17	52	14	44.6	9.1	108	19	53	18
9.647	86	17	42	14	35.5	8.7	89	19	43	15
10.37	69	16	34	15	27.8	8.8	69	18	34	12
11.14	54	15	28	14	21.7	9.1	54	18	28	10
11.97	43	14	22	13	16.6	9.0	42	17	22.9	9.4
12.86	35	13	19	12	13.5	8.8	33	17	20.0	8.8
13.82	29	13	17	13	11.3	8.2	27	15	18.0	8.1
14.86	25	13	16	12	9.7	7.4	24	15	17.0	8.1
15.96	23	13	15	11	8.2	6.9	21	14	16.7	8.8
17.15	22	13	14	11	7.8	7.5	19	14	16.7	9.2
18.43	21	14	8.6	7.6	3.1	3.5	18	13	12.4	8.6
19.81	1.6	1.1	-	-	-	-	-	-	-	-

Table 11. Sum of squared residuals from APS-derived respirable mass as a function of particle dynamic shape factor

Granite		Stone A		Stone B		Stone C	
χ (-)	S (μg^2)						
1	3860000	1	817000	1	1320000	1	8810000
1.1	3080000	1.1	561000	1.1	854000	1.1	6610000
1.2	2350000	1.2	343000	1.2	469000	1.2	4630000
1.3	1700000	1.3	174000	1.3	186000	1.3	2920000
1.4	1140000	1.4	65500	1.4	30100	1.4	1570000
1.5	689000	1.45	36800	1.425	12900	1.5	626000
1.6	374000	1.5	27300	1.4375	7600	1.55	339000
1.65	274000	1.55	37600	1.45	4680	1.6	178000
1.7	213000	1.6	70000	1.4625	4270	1.625	147000
1.725	200000	1.7	203000	1.475	6220	1.65	152000
1.7375	198000	1.8	435000	1.5	17800	1.675	194000
1.75	198000	1.9	784000	1.55	71700	1.7	272000
1.7625	201000			1.6	171000	1.8	973000
1.775	207000			1.7	508000	1.9	2340000
1.8	229000			1.8	1040000	2	4480000
1.9	438000			1.9	1820000		
2	858000						

Stone 1		Stone 2		Stone 3		Stone 4		Stone 5	
χ (-)	S (μg^2)								
1	128000	1	39200	1	12400	1	131000	1	31500
1.1	86600	1.1	21900	1.1	4990	1.1	79500	1.1	17600
1.2	52000	1.2	9560	1.15	2670	1.2	39200	1.2	7940
1.3	25400	1.25	5570	1.2	1410	1.3	12800	1.25	5030
1.4	8600	1.3	3230	1.225	1200	1.35	5750	1.3	3500
1.45	4380	1.325	2730	1.25	1290	1.4	3100	1.35	3500
1.5	3140	1.3375	2650	1.275	1690	1.45	5260	1.4	5170
1.55	5100	1.35	2690	1.3	2420	1.5	12400	1.5	13700
1.6	10400	1.3625	2860	1.4	8750	1.6	43500	1.6	30000
1.7	31900	1.375	3130	1.5	21200	1.7	98400	1.7	54900
1.8	69400	1.4	4080	1.6	40100	1.8	179000	1.8	89400
1.9	124000	1.5	13200	1.7	66800	1.9	291000	1.9	134000
2	198000	1.6	31400	1.8	101000			2	190000
		1.7	60200	1.9	145000				
		1.8	100000	2	198000				
		1.9	152000						
		2	219000						

Appendix IV. Respirable Sample Dataset

Table 12. Complete dataset of respirable samples with corresponding stone mass removed during grinding and grinding time

Stone	Run #	Sample #	Stone mass removed (g)	Grinding time (min)	Dust mass ($\mu\text{g sample}^{-1}$)	Dust LOD ($\mu\text{g sample}^{-1}$)	Dust LOQ ($\mu\text{g sample}^{-1}$)	Cristobalite mass ($\mu\text{g sample}^{-1}$)	Cristobalite LOD ($\mu\text{g sample}^{-1}$)	Cristobalite LOQ ($\mu\text{g sample}^{-1}$)	Quartz mass ($\mu\text{g sample}^{-1}$)	Quartz LOD ($\mu\text{g sample}^{-1}$)	Quartz LOQ ($\mu\text{g sample}^{-1}$)	Tridymite mass ($\mu\text{g sample}^{-1}$)	Tridymite LOD ($\mu\text{g sample}^{-1}$)	Tridymite LOQ ($\mu\text{g sample}^{-1}$)
Granite	1	S35	150	8	1700	40	130	0	90	300	380	5	17	0	10	33
Granite	1	S37	150	8	1600	40	130	0	80	300	360	5	17	0	10	33
Granite	2	S39	106	8	1800	40	130	0	90	300	480	5	17	0	10	33
Granite	2	S41	106	8	1700	40	130	0	90	300	450	5	17	0	10	33
Granite	3	S43	120	8	2200	40	130	0	100	330	550	10	34	0	10	33
Granite	3	S45	120	8	2100	40	130	0	100	330	510	10	34	0	10	33
Stone A	1	S23	85	8	1200	40	130	450	60	200	120	5	17	0	100	330
Stone A	1	S25	85	8	1000	40	130	430	60	200	110	5	17	0	100	330

EPHB Report No. 2023-DFSE-1489

Stone A	2	S27	97	8	1200	40	130	510	60	200	210	5	17	0	100	330
Stone A	2	S29	97	8	1200	40	130	470	60	200	210	5	17	0	100	330
Stone A	3	S31	81	8	890	40	130	410	30	100	170	5	17	0	60	200
Stone A	3	S33	81	8	770	40	130	320	30	100	150	5	17	0	60	200
Stone B	1	S11	122	8	1300	40	130	210	20	66	120	5	17	0	10	33
Stone B	1	S13	122	8	1300	40	130	220	20	66	120	5	17	0	10	33
Stone B	2	S15	135	8	1500	40	130	240	20	66	140	5	17	0	10	33
Stone B	2	S17	135	8	1400	40	130	250	20	66	120	5	17	0	10	33
Stone B	3	S19	154	8	1600	40	130	270	20	66	140	5	17	0	10	33
Stone B	3	S21	154	8	1500	40	130	270	20	66	140	5	17	0	10	33
Stone C	1	S1	150	8	1300	40	130	0	5	17	0	5	17	0	10	33
Stone C	2	S3	472	16	5200	40	130	0	5	17	0	5	17	0	10	33
Stone C	2	S5	472	16	3800	40	130	0	5	17	11 ^a	5	17	0	10	33
Stone C	3	S7	238	8	2900	40	130	0	5	17	0	5	17	0	10	33
Stone C	3	S9	238	8	2300	40	130	0	5	17	0	5	17	0	10	33
Stone 1	1	48	76	4	350	20	67	140	5	17	68	5	17	0	10	33
Stone 1	1	51	76	4	380	20	67	140	5	17	67	5	17	0	10	33
Stone 1	1	53	76	4	380	20	67	150	5	17	77	5	17	0	10	33
Stone 1	1	55	76	4	380	20	67	150	5	17	75	5	17	0	10	33
Stone 1	1	57	76	4	340	20	67	130	5	17	64	5	17	0	10	33
Stone 1	1	59	76	4	290	20	67	120	5	17	55	5	17	0	10	33
Stone 1	2	47	92	4.7	450	20	67	190	5	17	92	5	17	0	10	33
Stone 1	2	50	92	4.7	520	20	67	220	5	17	100	5	17	0	10	33
Stone 1	2	61	92	4.7	540	20	67	240	5	17	110	5	17	0	10	33
Stone 1	2	63	92	4.7	520	20	67	240	5	17	110	5	17	0	10	33
Stone 1	2	67	92	4.7	390	20	67	170	5	17	80	5	17	0	10	33
Stone 1	2	72	92	4.7	540	20	67	210	5	17	110	5	17	0	10	33
Stone 1	3	49	81	4	390	20	67	150	5	17	76	5	17	0	10	33
Stone 1	3	54	81	4	450	20	67	190	5	17	90	5	17	0	10	33
Stone 1	3	58	81	4	480	20	67	190	5	17	89	5	17	0	10	33
Stone 1	3	60	81	4	410	20	67	180	5	17	88	5	17	0	10	33
Stone 1	3	64	81	4	470	20	67	200	5	17	98	5	17	0	10	33
Stone 1	3	69	81	4	360	20	67	150	5	17	72	5	17	0	10	33
Stone 2	1	68	74	4	240	20	67	35	5	17	150	5	17	0	10	33
Stone 2	1	79	74	4	230	20	67	36	5	17	150	5	17	0	10	33
Stone 2	1	84	74	4	260	20	67	34	5	17	140	5	17	0	10	33
Stone 2	1	85	74	4	230	20	67	31	5	17	120	5	17	0	10	33
Stone 2	1	93	74	4	250	20	67	40	5	17	150	5	17	0	10	33
Stone 2	1	96	74	4	260	20	67	38	5	17	160	5	17	0	10	33
Stone 2	2	80	81	4	320	20	67	38	5	17	200	5	17	0	10	33
Stone 2	2	86	81	4	400	20	67	47	5	17	240	5	17	0	10	33
Stone 2	2	88	81	4	320	20	67	35	5	17	200	5	17	0	10	33

EPHB Report No. 2023-DFSE-1489

Stone 2	2	91	81	4	300	20	67	34	5	17	180	5	17	0	10	33
Stone 2	2	94	81	4	300	20	67	39	5	17	200	5	17	0	10	33
Stone 2	2	95	81	4	280	20	67	33	5	17	170	5	17	0	10	33
Stone 2	3	1	70	4	370	20	67	43	5	17	230	5	17	0	10	33
Stone 2	3	3	70	4	320	20	67	38	5	17	210	5	17	0	10	33
Stone 2	3	6	70	4	290	20	67	36	5	17	190	5	17	0	10	33
Stone 2	3	8	70	4	280	20	67	29	5	17	150	5	17	0	10	33
Stone 2	3	89	70	4	290	20	67	31	5	17	170	5	17	0	10	33
Stone 2	3	90	70	4	310	20	67	33	5	17	180	5	17	0	10	33
Stone 3	1	2	75	4	200	20	67	0	5	17	140	5	17	0	10	33
Stone 3	1	4	75	4	200	20	67	0	5	17	130	5	17	0	10	33
Stone 3	1	5	75	4	190	20	67	0	5	17	130	5	17	0	10	33
Stone 3	1	9	75	4	200	20	67	0	5	17	140	5	17	0	10	33
Stone 3	1	10	75	4	200	20	67	0	5	17	140	5	17	0	10	33
Stone 3	1	16	75	4	170	20	67	0	5	17	120	5	17	0	10	33
Stone 3	2	7	74	4	250	20	67	0	5	17	190	5	17	0	10	33
Stone 3	2	11	74	4	190	20	67	0	5	17	150	5	17	0	10	33
Stone 3	2	12	74	4	240	20	67	0	5	17	180	5	17	0	10	33
Stone 3	2	14	74	4	240	20	67	0	5	17	180	5	17	0	10	33
Stone 3	2	17	74	4	240	20	67	0	5	17	190	5	17	0	10	33
Stone 3	2	24	74	4	240	20	67	0	5	17	190	5	17	0	10	33
Stone 3	3	13	68	4	240	20	67	0	5	17	190	5	17	0	10	33
Stone 3	3	15	68	4	210	20	67	0	5	17	170	5	17	0	10	33
Stone 3	3	19	68	4	240	20	67	0	5	17	180	5	17	0	10	33
Stone 3	3	20	68	4	240	20	67	0	5	17	190	5	17	0	10	33
Stone 3	3	21	68	4	180	20	67	0	5	17	150	5	17	0	10	33
Stone 3	3	22	68	4	230	20	67	0	5	17	180	5	17	0	10	33
Stone 4	1	18	93	4	530	20	67	230	5	17	130	5	17	0	20	67
Stone 4	1	27	93	4	480	20	67	200	5	17	110	5	17	0	20	67
Stone 4	1	28	93	4	420	20	67	180	5	17	100	5	17	0	10	33
Stone 4	1	32	93	4	460	20	67	200	5	17	110	5	17	0	10	33
Stone 4	1	40	93	4	470	20	67	180	5	17	100	5	17	0	10	33
Stone 4	1	42	93	4	410	20	67	190	5	17	100	5	17	0	20	67
Stone 4	2	25	88	4	540	20	67	230	5	17	120	5	17	0	20	67
Stone 4	2	26	88	4	500	20	67	190	5	17	110	5	17	0	20	67
Stone 4	2	29	88	4	480	20	67	200	5	17	110	5	17	0	20	67
Stone 4	2	31	88	4	560	20	67	230	5	17	130	5	17	0	20	67
Stone 4	2	34	88	4	500	20	67	220	5	17	120	5	17	0	10	33
Stone 4	2	39	88	4	480	20	67	150	5	17	86	5	17	0	10	33
Stone 4	3	23	85	4	530	20	67	240	5	17	130	5	17	0	20	67
Stone 4	3	30	85	4	500	20	67	220	5	17	120	5	17	0	20	67
Stone 4	3	37	85	4	440	20	67	200	5	17	100	5	17	0	10	33

EPHB Report No. 2023-DFSE-1489

Stone 4	3	41	85	4	470	20	67	190	5	17	100	5	17	0	20	67
Stone 4	3	44	85	4	490	20	67	220	5	17	120	5	17	0	20	67
Stone 4	3	46	85	4	550	20	67	260	5	17	140	5	17	0	10	33
Stone 5	1	65	66	4	240	20	67	110	5	17	40	5	17	0	10	33
Stone 5	1	73	66	4	210	20	67	100	5	17	31	5	17	0	10	33
Stone 5	1	74	66	4	190	20	67	79	5	17	28	5	17	0	10	33
Stone 5	1	75	66	4	200	20	67	110	5	17	33	5	17	0	10	33
Stone 5	1	77	66	4	220	20	67	110	5	17	38	5	17	0	10	33
Stone 5	1	83	66	4	270	20	67	110	5	17	35	5	17	0	10	33
Stone 5	2	52	75	4	290	20	67	130	5	17	47	5	17	0	10	33
Stone 5	2	56	75	4	270	20	67	130	5	17	42	5	17	0	10	33
Stone 5	2	62	75	4	310	20	67	150	5	17	52	5	17	0	10	33
Stone 5	2	66	75	4	260	20	67	130	5	17	43	5	17	0	10	33
Stone 5	2	76	75	4	320	20	67	160	5	17	53	5	17	0	10	33
Stone 5	2	81	75	4	310	20	67	130	5	17	42	5	17	0	10	33
Stone 5	3	70	69	4	310	20	67	120	5	17	40	5	17	0	10	33
Stone 5	3	71	69	4	280	20	67	130	5	17	43	5	17	0	10	33
Stone 5	3	78	69	4	230	20	67	110	5	17	32	5	17	0	10	33
Stone 5	3	82	69	4	340	20	67	160	5	17	52	5	17	0	10	33
Stone 5	3	87	69	4	260	20	67	110	5	17	35	5	17	0	10	33
Stone 5	3	92	69	4	290	20	67	110	5	17	34	5	17	0	10	33

^aMass identified as an outlier as this was below the LOQ and the only sample from Stone C (including bulk material, bulk dust, respirable dust, total dust, and size-classified dust samples) with detectable crystalline silica

**Delivering on the Nation's promise:
Promoting productive workplaces through
safety and health research**

Get More Information

Find NIOSH products and get answers to workplace safety and health questions:

1-800-CDC-INFO (1-800-232-4636) | TTY: 1-888-232-6348

CDC/NIOSH INFO: [cdc.gov/info](https://www.cdc.gov/info) | [cdc.gov/niosh](https://www.cdc.gov/niosh)

Monthly *NIOSH eNews*: [cdc.gov/niosh/eNews](https://www.cdc.gov/niosh/eNews)